

A FINITE ELEMENT APPROACH FOR ANALYSIS OF DAMPING
CAPABILITIES OF POLYMER COMPOSITES.

by

Satyam Shukla

A thesis submitted to the faculty of
The University of North Carolina at Charlotte
in partial fulfillment of the requirements
for the degree of Master of Science in
Mechanical Engineering

Charlotte

2020

Approved by:

Dr. Alireza Tabarraei

Dr. Ronald E. Smelser

Dr. Navid Goudarzi

©2020
Satyam Shukla
ALL RIGHTS RESERVED

ABSTRACT

SATYAM SHUKLA. A finite element approach for analysis of damping capabilities of polymer composites. . (Under the direction of DR. ALIREZA TABARRAEI)

Mechanical vibrations are a part of several industrial equipment, machinery, systems and vehicles being used in our day to day life. Damping of such unwanted vibrations have been of utmost importance for several industrial operations. Polymer composites have proven to be an effective solution for damping of such vibrations. This study uses finite element methods to analyze the effect of change in key influential parameters on the damping capability of the polymer composite models. The damping capability is measured in terms of 'loss factor' $\tan \delta$ which can be expressed as the ratio of loss to storage modulus of the composite model. Finite element software ABAQUS is used for modelling the polymer composites. This study analyzes the damping properties of two types of polymer composites. The first polymer composite model is made of spherical elastic inclusions dispersed in a cubical viscoelastic matrix. The composite model also consists of a viscoelastic interphase region between the spherical inclusions and the matrix. The finite element model is subjected to mixed boundary conditions and a normal strain is applied on one of the faces. The damping properties are studied over a range of vibration frequency from $10^{-8}/s$ to $10^2/s$. The study analyzes the effect of interphase region, volume fraction of inclusions and loading frequency on overall damping capability of the composite model.

The second part of the study analyzes the damping properties of a model with sinusoidal carbon nanotube as inclusions dispersed in a cuboidal viscoelastic matrix. The finite element model is again subjected to mixed boundary conditions with a normal strain acting on one of the faces with frequency ranging from a $10^{-8}/s$ to $10^2/s$. The effect of change in input parameters like waviness of nanotube inclusions ,volume fraction and loading frequency is studied. A sensitivity analysis is conducted

to understand how the peak damping capability is effected by change in input parameters of composite material properties. Sensitivity analysis is conducted on second model with nanotube inclusions inside a viscoelastic matrix. The elastic modulus of inclusions and matrix is varied within a pre-decided range while keeping the boundary and loading conditions same.

ACKNOWLEDGEMENTS

I would like to thank my advisor Dr. Alireza Tabarraei at University of North Carolina at Charlotte. The door to Prof. Tabarraei's office was always open whenever I ran into a difficulty or had a question, during the course of my research. He consistently steered me in the right the direction whenever he thought I needed it. I would like to thank my committee members Dr. Ronald E. Smelser and Dr. Navid Goudarzi for their guidance. I would also like to thank my parents for their love and support, my friends Akshith Subramanian, Pauras Sawant, Wilfred Tuscano and many others for lifting me up when I felt low.

TABLE OF CONTENTS

LIST OF FIGURES	viii
LIST OF TABLES	x
CHAPTER 1: INTRODUCTION	1
CHAPTER 2: THESIS PROBLEM AND APPROACH	7
2.1. Polymer Composite With Spherical Elastic Inclusions In A Viscoelastic Matrix	7
2.1.1. Problem	7
2.1.2. Approach	7
2.1.3. Effect of Frequency	8
2.1.4. Effect of Volume Fraction	9
2.1.5. Effect of Interphase	9
2.1.6. Effect of Inclusion Distribution or Arrangement	9
2.2. Polymer Composite With Carbon Nanotube Inclusions In A Viscoelastic Matrix	9
2.2.1. Problem	9
2.2.2. Approach	10
2.2.3. Effect of Waviness	10
2.2.4. Effect of Volume Fraction	11
2.2.5. Effect of Loading Frequency	11
CHAPTER 3: MATERIAL MODEL	12
3.0.1. Matrix Material	12
3.0.2. Spherical Elastic Inclusions	15

	vii
3.0.3. Interphase	15
3.0.4. Carbon Nanotube Inclusion Material	15
CHAPTER 4: FINITE ELEMENT MODEL	16
4.1. Composite with Spherical Inclusions	17
4.1.1. Random sequential absorption	19
4.1.2. Boundary and Loading Conditions	21
4.2. Composite with Carbon Nanotube Inclusions	22
4.2.1. Boundary and Loading Conditions	23
CHAPTER 5: RESULT AND DISCUSSION	25
5.1. Polymer Composite with Spherical Inclusions	25
5.1.1. Effect of Volume Fraction	25
5.1.2. Effect of Interphase	28
5.1.3. Ensemble Averaging	28
5.2. Carbon Nanotube Polymer Composite	29
5.2.1. Effect of Waviness	30
5.2.2. Effect of Volume Fraction	32
5.3. Sensitivity Analysis	35
CHAPTER 6: CONCLUSION	40
REFERENCES	42

LIST OF FIGURES

FIGURE 1.1: Two Dimensional Representation of RVE With Spherical Inclusions	3
FIGURE 1.2: Two Dimensional Representation of RVE With Nanotube Inclusions	4
FIGURE 2.1: 3 D representation of polymer matrix with glass inclusions.	8
FIGURE 2.2: Schematics of modeling parameters for inclusions with waviness 0.05	11
FIGURE 4.1: Phase lag between input strain wave and output stress wave [1].	17
FIGURE 4.2: 3 D meshing of polymer matrix with spherical inclusions.	18
FIGURE 4.3: Interphase mesh.	18
FIGURE 4.4: Inclusion mesh .	18
FIGURE 4.5: Flow chart for random sequential absorption technique.	20
FIGURE 4.6: Boundary conditions for model with spherical inclusions.	21
FIGURE 4.7: Boundary conditions for polymer with nanotube inclusions.	24
FIGURE 5.1: $\tan \delta$ for Volume Fraction 5%	26
FIGURE 5.2: $\tan \delta$ for Volume Fraction 10%	27
FIGURE 5.3: $\tan \delta$ for Volume Fraction 15%	27
FIGURE 5.4: Comparison of peak $\tan \delta$ with and without interphase against volume fraction	28
FIGURE 5.5: Ensemble Averaging for polymer with 5% volume fraction.	29
FIGURE 5.6: $\tan \delta$ response with 5% volume fraction.	30
FIGURE 5.7: $\tan \delta$ response with 10% volume fraction.	31
FIGURE 5.8: $\tan \delta$ response with 15% volume fraction.	31

FIGURE 5.9: $\tan \delta$ response for 0.05 waviness against all volume fraction.	32
FIGURE 5.10: $\tan \delta$ response for 0.1 waviness against all volume fraction.	33
FIGURE 5.11: $\tan \delta$ response for 0.2 waviness against all volume fraction.	34
FIGURE 5.12: Comparison of peak $\tan \delta$.	34
FIGURE 5.13: Sensitivity analysis against matrix modulus for volume fraction 5% and 0.05 waviness.	37
FIGURE 5.14: Sensitivity analysis against inclusion modulus for volume fraction 5% and 0.05 waviness.	37
FIGURE 5.15: Sensitivity analysis against matrix modulus for volume fraction 5% and 0.1 waviness.	38
FIGURE 5.16: Sensitivity analysis against inclusion modulus for volume fraction 5% and 0.1 waviness.	38
FIGURE 5.17: Sensitivity analysis against matrix modulus for volume fraction 5% and 0.2 waviness.	39
FIGURE 5.18: Sensitivity analysis against inclusion modulus for volume fraction 5% and 0.2 waviness.	39

LIST OF TABLES

TABLE 3.1: Relaxation moduli and relaxation time for matrix material [2]	14
TABLE 4.1: Dimension and mesh size of RVE	19
TABLE 4.2: SWCNT Polymer Matrix Parameters [3]	23
TABLE 5.1: Parameter range for sensitivity analysis.	35

CHAPTER 1: INTRODUCTION

Although beneficial in some cases, vibrations are mainly a source of energy loss and inaccuracy in various systems and machinery. Over time, many attempts have been made to deal with such unwanted vibrations. Polymer composites have proven to be an effective solution for damping of vibrations. Viscoelastic polymer composites are widely used for damping of vibrations in several industrial areas. One of the primary reasons for effectiveness of polymer composites as damping agents is due to the viscoelastic nature of the matrix. As the name suggests, viscoelastic materials possess both viscous and elastic properties. The dual nature of the matrix plays an important role in the damping of the vibrations, specially in automotive, aerospace, civil engineering etc. Roeder and Stanton [4] studied the use of elastomeric bearings by structural engineers in wide variety of areas. Their primary aim was to understand the behaviour of these elastomeric bearings, their failure modes and design processes to spread more knowledge among the structural designers using these bearings. Such bearings were used in bridges to accommodate creep and thermal expansions. They were also used for seismic pad isolation and damping of machinery vibrations.

Rao [5] studied the application of viscoelastic damping in automotive and aerospace industry. Damping of vibrations can be classified into three main categories as active, passive and semi-active damping. Active damping involves use of speakers, actuators and microprocessors to produce an out of phase sound wave to cancel out the noise. In his study, Rao focused on the passive damping methods. These methods involve use of viscoelastic damping materials to reduce vibrations using free layer damping and constraint layer damping. He also studied the recent technological advancements which use a combination of these techniques for cancellation of noise and structural

vibrations. Tsai [6] studied the use of viscoelastic materials in construction industry. He studied the energy absorbing behaviour and capacities of the viscoelastic dampers. Duncan [7] studied the applications of polymer composites and nano-composites being used in the food packaging industry.

One of the major advantages of using polymer composites in damping processes is the freedom of tweaking its properties depending upon the area of usage. Fillers are added to the matrix to increase the strength and stiffness of the composite. The desired properties of the polymer composites can be achieved by tweaking the shape, size, volume fraction, stiffness etc. of the fillers and matrix. Various attempts have been made in the past to study how change in inclusion properties changes damping properties of the polymer composite. Adam and Bacon [8] studied the effect of fiber orientation in a fiber reinforced plastic. They developed a micro-mechanical model to study the effect of orientation on the flexural and torsional damping along with the modulus of the polymer composite. Hwang and Gibson [9] proposed a finite element method to model the damping and stiffness of discontinuous fiber reinforced plastic. Kaliske and Rothert [10] derived an analytical method to determine the damping properties of the polymer composites. One of the main highlights of their work was the derivation of six damping coefficients for six different stress components.

Brinson and Lin [2] used the homogenization techniques developed by Mori - Tanaka and Halpin Tsai [11] for determining the loss and storage modulus of a fiber reinforced composite. The ratio of loss to storage modulus is referred to as $\tan\delta$. Brinson and Lin used this technique on a composite with single inclusion. As the number of inclusion increased, the accuracy of their results reduced. Kulkarni [12] studied the damping properties of filled elastomers and how it is affected by factors like inclusion property and volume fraction. Kulkarni [13, 14] also studied the damping properties of elastomers through wave propagation along with wave attenuation characteristics of epoxy polymer composites.

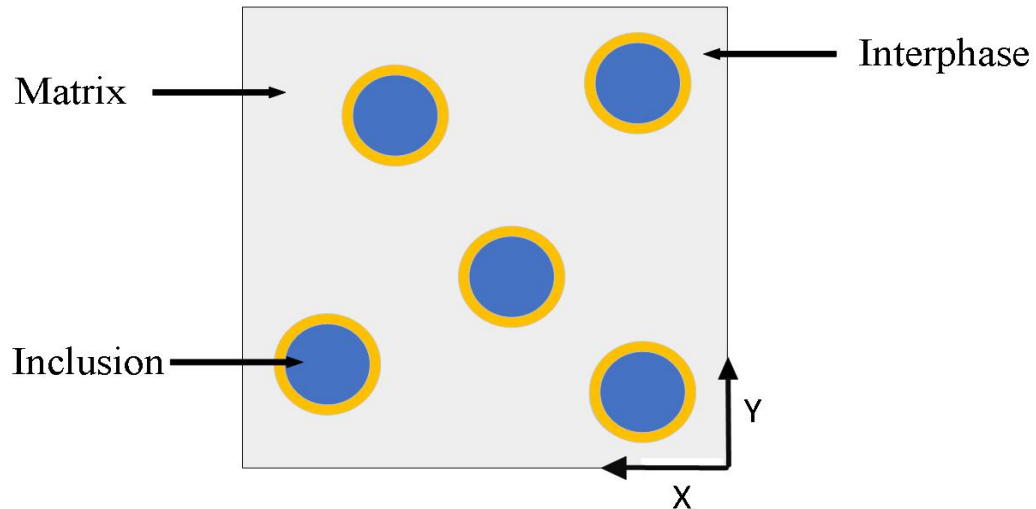


Figure 1.1: Two Dimensional Representation of RVE With Spherical Inclusions

Apart from inclusions and matrix, several polymer composites consist of a third region known as interphase. The interphase region can be considered as a thin layer present where the inclusions come in contact with the matrix. Due to considerable difference in the properties of inclusions and matrix, the properties of interphase region can be significantly different than that of inclusions and matrix. Presence of interphase region may pose a problem in accurate prediction of properties of polymer composites. Brinson and Fisher [15] studied the prediction of mechanical properties of multi-phase viscoelastic materials. They used the Mori - Tanaka method and its extension developed by Banviste to compare the predictions of moduli and impact of interphase regions in polymer matrix composites.

The first part of the study determines the damping capability of polymer composites and how it is affected by presence of interphase region. The matrix is in shape of a cube with each side equal to 0.3 mm. The spherical elastic inclusions are dispersed in the matrix using Random Sequential Absorption (RSA) technique. Figure 4.5 shows the algorithm used for dispersing the inclusions in a matrix. A detailed explanation of the technique is given in later sections. The interphase region is modelled as a

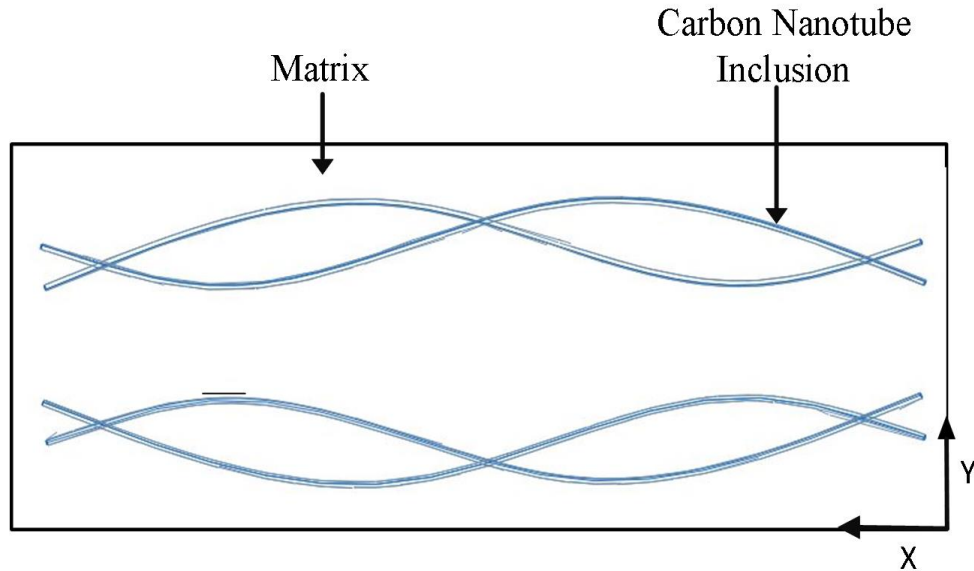


Figure 1.2: Two Dimensional Representation of RVE With Nanotube Inclusions

thin hollow spherical shell surrounding the solid spherical inclusions. The interphase region is considered to be viscoelastic in nature with elastic modulus lower than that of the elastic inclusion but higher than the matrix.

Commercial finite element software ABAQUS by Dassault Systems is used for modelling and simulations. To accurately predict the response of the polymer composites, a representative volume element (RVE) is modeled. RVE is the smallest volume whose properties represent the properties of whole model. This study analyzes the effect of interphase region on the overall damping properties of the polymer model. It also compares the results with the damping properties of the polymer with no interphase region.

The second part of the study aims at determining the damping capability of a polymer composite model with carbon nanotubes as inclusions in a viscoelastic matrix. Figure 1.2 is the RVE representation of polymer with carbon nanotube inclusions. Carbon nanotube composites are one of the most widely used composites for various industrial applications. They have a set of extra ordinary mechanical properties which

make them one of the highly sought-after option. Their high strength to weight ratio, stiffness to weight ratio and high geometric aspect make them a suitable choice for wide range of applications [16, 17, 18]. The mechanical abilities of the carbon nanotube composites depend on several factors. One of the main factors is the bonding between the matrix and the dispersed nanotubes. Pantano[3] suggested that these dispersed nanotubes in the matrix can act as a reinforcing component for the composites. Also, at the same time these nanotubes can act as holes or cavities in the composite which can hamper the mechanical properties of the structure. Carbon nanotubes can be classified into two categories, single wall carbon nanotubes and multi wall carbon nanotubes. Attempts have been made to study the effects of nanotube inclusion as inclusion in polymer matrix on physical properties of the model. Pantano[3] analyzed the effect of multi wall carbon nanotube curvature and interface interaction of the composite on the overall composite stiffness. Andrew [19] used mixing to produce a multi wall carbon nanotubes (MWCNT) with 5 % volume fraction and obtained a 15 % increase in the overall composite stiffness as compared to that of just the matrix. Xia[20] analyzed a polypropylene MWCNT composite. An 8.8 % increase in stiffness composite was observed for 3 % weight MWCNTs. Song [21] also obtained similar results for an epoxy composite. 17 % increase in elastic composite was obtained for a 1.5 % wt MWCNTs. Models like [22, 23, 24] studied the stiffening effect of MWCNT inclusions in polymer matrix.

The second part of the study aims at determining the damping properties of a composite model with viscoelastic matrix and elastic carbon nanotubes as inclusions. The inclusions are in shape of a hollow single wall sinusoidal carbon nanotubes (SWCNT) dispersed in the matrix. The geometry for the RVE is taken from Pantanos [3] model in which the carbon nanotubes are dispersed like sinusoidal waves in the matrix. The matrix material chosen for this study is viscoelastic in nature. This study analyzes the damping capability of the model with carbon nanotubes as inclusions and how it

is affected by change in parameters like inclusion volume fraction, inclusion waviness and loading frequency. Damping capability of the model is analysed using the same finite element methods as for the previous model with spherical inclusions. Mixed boundary conditions are applied to the model with normal strain on one of the faces of the matrix. The aim is to determine the effect of waviness, volume fraction and loading frequency on damping capability of the composite model. The waviness of the carbon nanotubes is altered by altering the amplitude of the sinusoidal shaped inclusions.

In the last part of the study, a sensitivity analysis is performed for carbon nanotube polymer composite models with 5% inclusion volume fraction and waviness of 0.05, 0.1 and 0.2. This sensitivity analysis studies the effect of change in parameters like elastic modulus of inclusions and matrix on the damping capability of the polymer composite. Latin hypercube sampling technique is used to generate a sample set of Young's moduli within a pre-decided range. Peak damping capability is calculated for different combinations of elastic modulus of matrix and inclusions. The sensitivity analysis compares the results and analyzes how the change in modulus affects the damping capability of the carbon nanotube polymer composite model.

CHAPTER 2: THESIS PROBLEM AND APPROACH

In this section, thesis problem and the approach to towards its solution is presented. This thesis consists of two parts. The overall theoretical approach to solve both the parts is fundamentally same but the model geometry is different. Both model and the approach is presented in the sections below.

2.1 Polymer Composite With Spherical Elastic Inclusions In A Viscoelastic Matrix

2.1.1 Problem

In this part of the study, damping capability of a polymer composite with spherical glass inclusions in a viscoelastic matrix is analyzed. The polymer model has three parts, the matrix, the inclusions and the interphase layer between the matrix and the inclusions. The aim is to determine the effect of interphase region on the damping capability of the polymer. The effect of change in volume fraction and loading frequency is also studied.

2.1.2 Approach

The study uses principles of finite element to solve the problem at hand. Commercial finite element software ABAQUS by Dassault Systems is used for modelling and analysis. The RVE is subjected to set of mixed boundary conditions and a normal strain is applied on one of the faces. The matrix material is modeled as a homogeneous viscoelastic material. The inclusions are in shape of a solid sphere and material is elastic in nature. The interphase region is also modeled as a spherical shell around the solid elastic inclusion. Interphase is viscoelastic in nature with modulus higher than that of the matrix but lower than of inclusions. The inner radius of an inter-

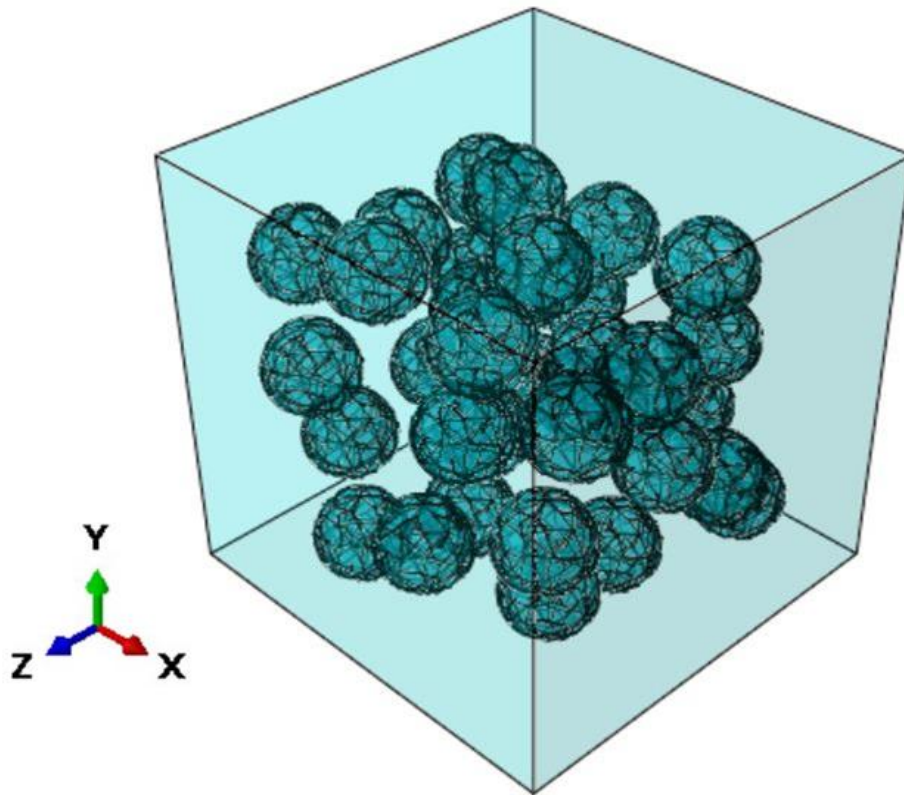


Figure 2.1: 3 D representation of polymer matrix with glass inclusions.

phase shell is equal to the outer radius of the inclusion its surrounding with center of origin same for both. Both inclusions and interphase shells are dispersed in the matrix using Random Sequential Absorption technique. Figure 2.1 represents the 3D matrix with 15% glass inclusion volume fraction.

2.1.3 Effect of Frequency

The finite element model is subjected to a normal strain on one face with frequency ranging from $10^{-8}/s$ to $10^2/s$. The study analyzes the damping response of the polymer composite model over this range of frequency.

2.1.4 Effect of Volume Fraction

The volume fraction is calculated as the ratio of total volume of inclusions over volume of the matrix. Volume fraction is increased by introducing more inclusions in the matrix. Volume fraction can be calculated as,

$$\text{Volume fraction} = \frac{n \times \text{Vol}_{\text{inclusion}}}{\text{Vol}_{\text{matrix}}} \quad (2.1)$$

This study analyzes the effect of volume fraction on the damping properties of the composite model. Three models with volume fraction 5% , 10% and 15% are analysed.

2.1.5 Effect of Interphase

The interphase is modelled as a thin shell of viscoelastic material surrounding the elastic inclusion with center of origin for both being same. Thickness of the interphase region is taken to be 0.001 mm. This study analyzes the effect of interphase region on the overall damping capability of the polymer composite.

2.1.6 Effect of Inclusion Distribution or Arrangement

The elastic inclusions are randomly distributed in the matrix using Random Sequential Absorption Technique (RSA). To minimise the impact of randomness, the damping properties are studied on several model RVE with same volume fraction but different inclusion arrangement. Peak damping capability is calculated for each instance. The variation in peak damping capability with increasing number of instances is studied.

2.2 Polymer Composite With Carbon Nanotube Inclusions In A Viscoelastic Matrix

2.2.1 Problem

The second part studies the damping capability of a polymer composite model with single wall carbon nanotubes as inclusions. The nanotubes are modelled as sinusoidal

tubes of radius 5 nm using the ABAQUS shell element. The study analyzes the effect of inclusion and its waviness on the damping capability of the model. The study also analyzes the effect of change in volume fraction and loading frequency on the damping capability of the model.

2.2.2 Approach

The study uses principles of finite element to analyze the damping properties of the composite model. Commercial software ABAQUS by Dassault Systems is used for modelling and analysis. A representative volume element (RVE) is created which has sinusoidal nanotube inclusions inserted in a cuboidal viscoelastic matrix. This RVE is subjected to a set of mixed boundary conditions, with normal strain with vibration frequency ranging from 10^{-8} /s to 10^2 /s acting on one of the faces. The waviness of the nanotubes is calculated as a ratio of amplitude and wavelength . Table ?? lists all the parameters used to model the nanotube composite. The elastic modulus of a carbon nanotube ranges from 10^6 MPa to 10 TPa depending on the arrangement and number of walls. For this study, the elastic modulus and density of the nanotubes are chosen to be 1 TPa & 1 gr/cm^3 respectively.

2.2.3 Effect of Waviness

The study analyzes how the damping properties of the polymer composite model is changed upon changing the waviness of the nanotube inclusions. Three models are created, each with nanotube inclusion 0.05, 0.1 and 0.2. The figure 2.2 shows the parameters 'a' and ' λ ' for the nanotube inclusions. Here 'a' represents the amplitude and ' λ ' is the wavelength.

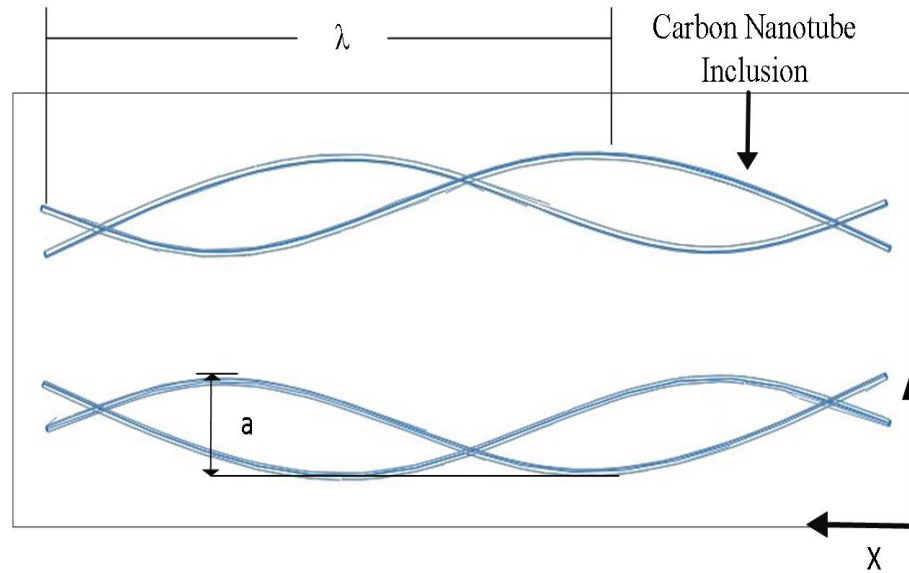


Figure 2.2: Schematics of modeling parameters for inclusions with waviness 0.05

2.2.4 Effect of Volume Fraction

Volume fraction of the carbon nanotube inclusions is varied by introducing more inclusions of same waviness. Affect of volume fraction the damping capability of the polymer model is analysed.

2.2.5 Effect of Loading Frequency

The finite element model of the polymer composite is subjected to a set of mixed boundary conditions. One of the faces of the model is subjected to a normal strain. The loading frequency is varied from $10^{-8}/s$ to $10^2/s$. The study analyzes the affect of this change in loading frequency on the damping capability of the polymer composite.

CHAPTER 3: MATERIAL MODEL

Constitutive equations form the basis of predicting material behaviour. Constitutive equations can be defined as the relation between any two parameters or physical quantities which defines the behaviour of the material when put under stress. Such equations are widely used in engineering and physics and are very important in achieving accurate results in finite element study. One example of such equations is the widely used Hooke's Law used for predicting the elastic behaviour of materials.

3.0.1 Matrix Material

The matrix of the polymer composite in this study is modeled to exhibit viscoelastic properties. This viscoelastic nature of the matrix imparts a high loss over storage bulk modulus which is referred to as 'loss factor'. When such materials are put under stress their deformation exhibits both viscous and elastic behaviour. The viscous part deforms slowly under stress while the elastic part tends to return to original state upon relaxation. In case of viscoelastic materials, the stress vs strain curve is in form of a hysteresis loop, the area under which represents energy loss. This energy loss is the reason why viscoelastic materials have good damping capabilities. There are several relations which will help in understanding the behaviour of such materials. The viscoelastic response of the material can be analysed as a complex modulus of elasticity and their ration. The constitutive relation for a visco elastic material is,

$$\sigma_{ij}(t) = \int_0^t C_{ijkl}(t - \tau) \frac{d\epsilon_{kl}(\tau)}{d\tau} d\tau, \quad (3.1)$$

where σ_{ij} denotes the stress tensor and ϵ_{kl} denotes the strain tensor. C_{ijkl} is the time dependent modulus for the matrix material. The following equation,

$$\sigma_{ij}(t) = \int_0^t 2G(t-\tau) \frac{d\epsilon_{ij}}{d\tau} d\tau + I \int_0^t K(t-\tau) d\epsilon_{ij}^{Vol} d\tau, \quad (3.2)$$

represents the linear viscoelastic material. Here ϵ_{ij} is deviatoric strain, ϵ_{ij}^{Vol} is the volumetric strain, $G(t)$ is the shear relaxation modulus and $K(t)$ is the bulk relaxation modulus. By applying a harmonic time deformation, represented by,

$$u_i(x, t) = u_i^0(x, \omega) e^{i\omega t}, \quad (3.3)$$

the strain field can be represented as ,

$$\epsilon_{ij}(x, t) = \epsilon_{ij}^0(x, \omega) e^{i\omega t}, \quad (3.4)$$

where x is the position vector and ω is the frequency. Using equation 3.4 in the original relation for viscoelastic material given by equation 3.2, the expression for deviatoric and dilatational stress components can be stated as,

$$S_{ij} = 2G^*(\omega) \epsilon_{ij}, \quad (3.5)$$

and

$$\sigma_{kk} = 3K^*(\omega) \epsilon_{kk}, \quad (3.6)$$

respectively.

Here, G^* and K^* are shear and bulk modulus. They can be defined in complex form

Table 3.1: Relaxation moduli and relaxation time for matrix material [2]

τ_{jG}	G_j	τ_{jG}	G_j
0.032	2.512	100.0	19.953
0.100	10.0	316.228	12.589
0.316	56.234	1000.0	2.512
1.0	316.228	3162.278	1.698
3.162	1000	10000.0	1.202
10.0	199.526	31622.777	1.148
31.623	50.119	100000.0	1.096
τ_{jK}	K_j	τ_{jK}	K_j
100	3000	316.228	100
$G_\infty = 3.162$	$K_\infty = 200$		

as ,

$$\begin{aligned}
 G^*(\omega) &= G'(\omega) + iG''(\omega), \\
 K^*(\omega) &= K'(\omega) + iK''(\omega),
 \end{aligned}
 \tag{3.7}$$

where G', K' are shear and bulk storage modulus and G'', K'' are shear and bulk loss modulus respectively. The storage modulus represents the ability of the material to store energy while the loss modulus represents the loss in energy. The ratio of the loss to storage modulus is defined as,

$$\tan\delta = \frac{G''}{G'}
 \tag{3.8}$$

Prony 3.1 series can be used to represent the shear and bulk modulus of the viscoelastic material as,

$$A(t) = A_\infty + \sum_{j=1}^N A_j e^{\frac{-t}{\tau_j}},
 \tag{3.9}$$

where A_j is the relaxation modulus, τ_j is the relaxation time and A_∞ is the long term relaxation modulus. 3.1 lists out the relaxation time and modulus used for this analysis. The density of the matrix chosen to be 1.0 gr/cm³ and elastic modulus as 9.4 MPa.

3.0.2 Spherical Elastic Inclusions

The elastic inclusions modeled for the study have a Young's modulus of 64 GPa which is significantly higher than the matrix modulus. The density of the inclusions is 2.47 gr/cm³.

3.0.3 Interphase

The interphase is modeled as a thin layer surrounding the inclusions. The interphase is viscoelastic in nature with elastic modulus as 29.8 MPa and density 1 gr/cm³. Thickness of the interphase shell is 0.001 mm. The visco elastic nature of the interphase material is again modeled using the same constitutive equations and prony series parameters.

3.0.4 Carbon Nanotube Inclusion Material

The carbon nanotube inclusions have an elastic modulus of 1 TPa which is much higher than that of the viscoelastic matrix . The nanotubes are modeled as thin homogeneous ABAQUS shell elements with density as 1.0 gr/cm³.

CHAPTER 4: FINITE ELEMENT MODEL

The finite element modeling approach for this study is divided into two parts. The first part deals with the modeling and analysis of a composite made up of elastic spherical inclusions dispersed in a visco elastic matrix. The second part explains the modeling of carbon nanotube polymer composite which has sinusoidal carbon nanotubes as inclusions dispersed in a viscoelastic matrix. Both models are subjected to same boundary conditions and periodic loading to study their damping capabilities.

To calculate the damping capability of the polymer composites, $\tan\delta$ is used as the measuring parameter. It is the ratios of loss to storage modulus and is also referred to as 'Loss Factor'. A normal strain is applied on one of the faces of RVE. This strain can be represented by the equation,

$$\epsilon_{yy} = \epsilon^0 \sin(\omega t). \quad (4.1)$$

Here, ϵ^0 is the amplitude of the applied strain, ω is the angular frequency and t is time. When a strain curve is applied to a viscoelastic material, a phase lag occurs between the input strain curve and the output stress curve. The difference in the phase is used to calculate $\tan \delta$. An example of phase lag between the input strain curve and output stress curve is shown in figure 4.1. The value of phase lag δ is related to the time lag that occurs between the input strain and the output stress wave as,

$$\delta = \omega \Delta t, \quad (4.2)$$

where Δt is time lag and ω is angular frequency. The amplitude ϵ^0 has no effect on

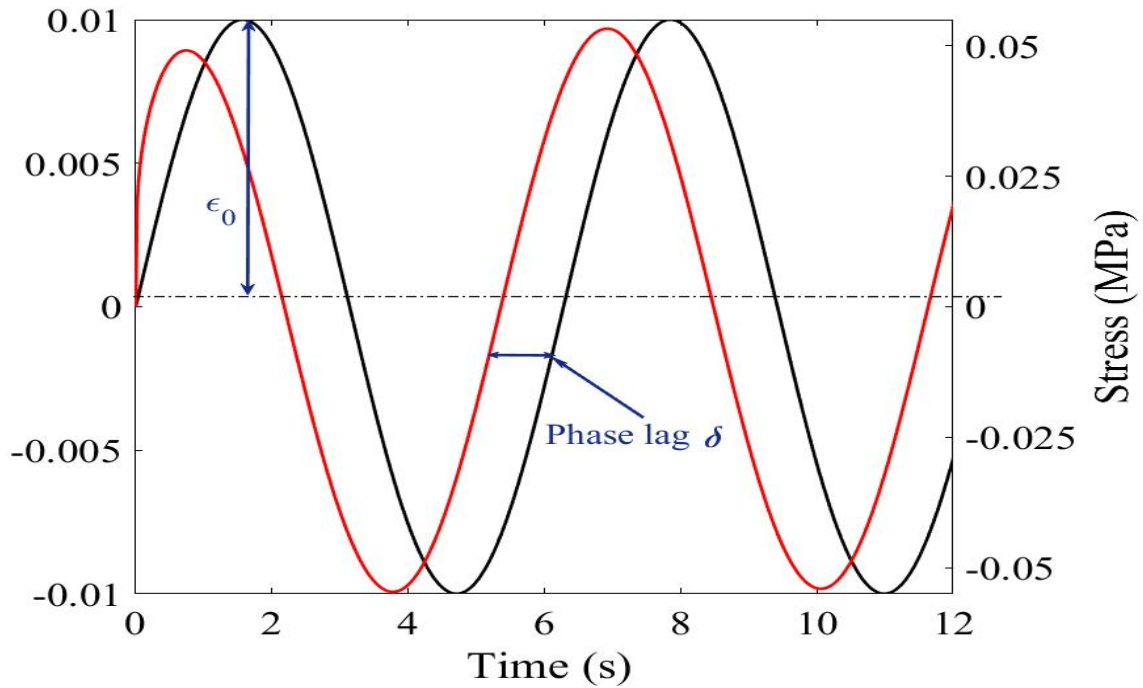


Figure 4.1: Phase lag between input strain wave and output stress wave [1].

the value of $\tan \delta$. An amplitude of 10 nm and 10 nm is chosen for the model with spherical inclusions and nanotube inclusions respectively.

4.1 Composite with Spherical Inclusions

A commercial software Abaqus is used for modeling and solution of the problem. These spherical inclusions with interphase shells are randomly dispersed in the matrix. As explained earlier, this study uses random sequential absorption (RSA) technique for distributing the inclusions and interphase within the matrix. The shape of the matrix is chosen to be that of a cube with each side equal to 0.3 mm. The inclusion are in shape of solid sphere with a radius of 0.03 mm.

The interphase is modeled in shape of a thin hollow sphere or shell. The interphase shell has an inner radius equal to the outer radius of the spherical inclusion and a thickness of 0.001 mm. The inner surface of the interphase is in contact with the outer surface of the spherical inclusion and the outer surface of the interphase is in contact with the matrix. The center of origin for both the interphase and the

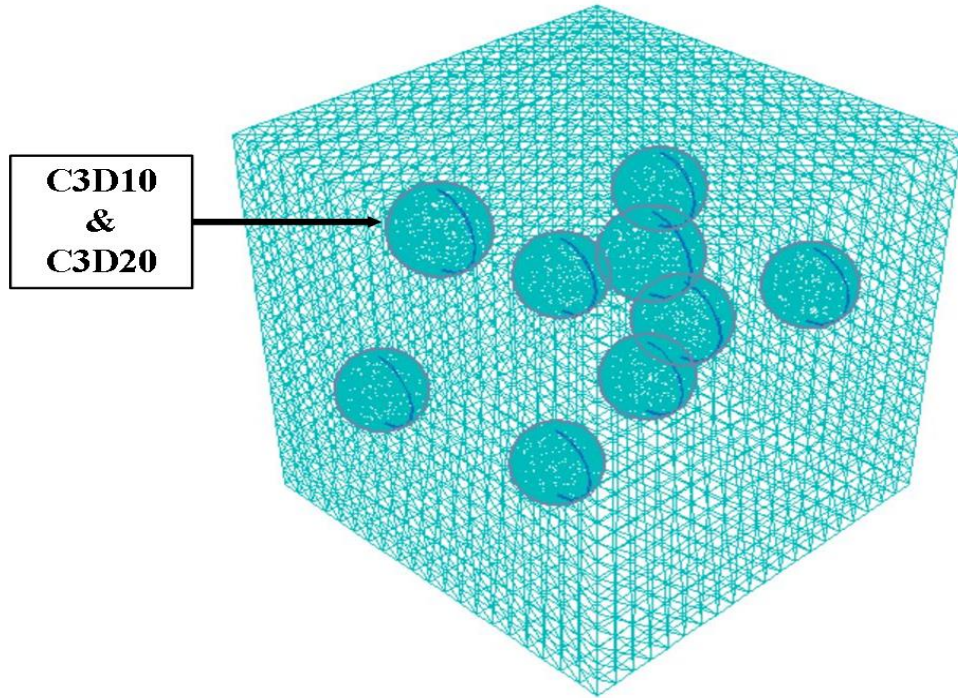


Figure 4.2: 3 D meshing of polymer matrix with spherical inclusions.

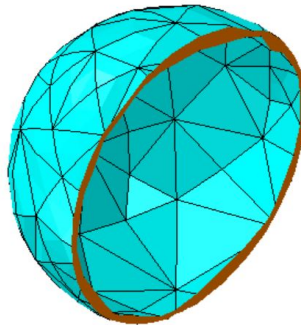


Figure 4.3: Interphase mesh.

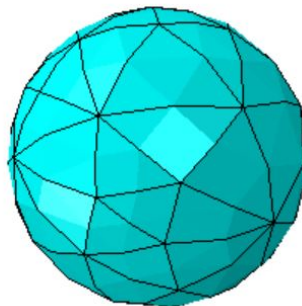


Figure 4.4: Inclusion mesh .

Table 4.1: Dimension and mesh size of RVE

Instance	Dimension	Seed Size
Matrix	0.3 x 0.3 x 0.3 mm ³	0.015
Inclusion	Rad = 0.03 mm	0.015
Interphase	Rad = 0.031 mm	0.0015

spherical inclusion is same. The spherical inclusions and the interphase shells are kept in position within the matrix by using the 'tie' function in ABAQUS. This function ties the common nodes of the surfaces in contact. The outer surface of the inclusion is tied with the inner surface of the interphase shell. The outer surface of the interphase shell is in turn tied with the viscoelastic matrix surrounding it.

4.1.1 Random sequential absorption

The first composite model under study has solid spherical inclusions surrounded by their respective hollow spherical shell, dispersed randomly in a cubical matrix. This study uses random sequential absorption technique for inserting the inclusion and the interphase in the matrix. Figure 4.5 represents a flow chart of RSA technique. The first inclusion point is randomly created within the matrix. An inclusion is introduced in the matrix and the volume fraction is calculated. If the volume fraction is less than desired, second inclusion is introduced at one more random point in the matrix. The distance between the new and old inclusions is calculated to satisfy a minimum distance criteria and avoid intersection. The volume fraction is again calculated to know if the desired value is achieved. This technique is used to generate model RVEs with different inclusion distribution while keeping the volume fraction same. It will be useful in analysing the impact of randomness in inclusion distribution on the damping capability of the model. This study applies python scripting in ABAQUS [25] for generating the RVE.

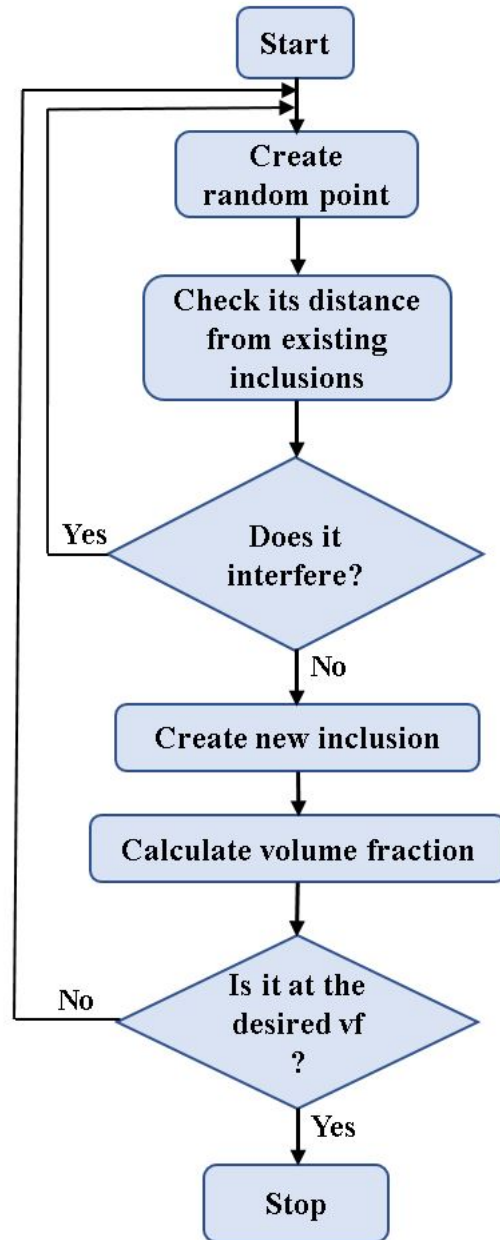


Figure 4.5: Flow chart for random sequential absorption technique.

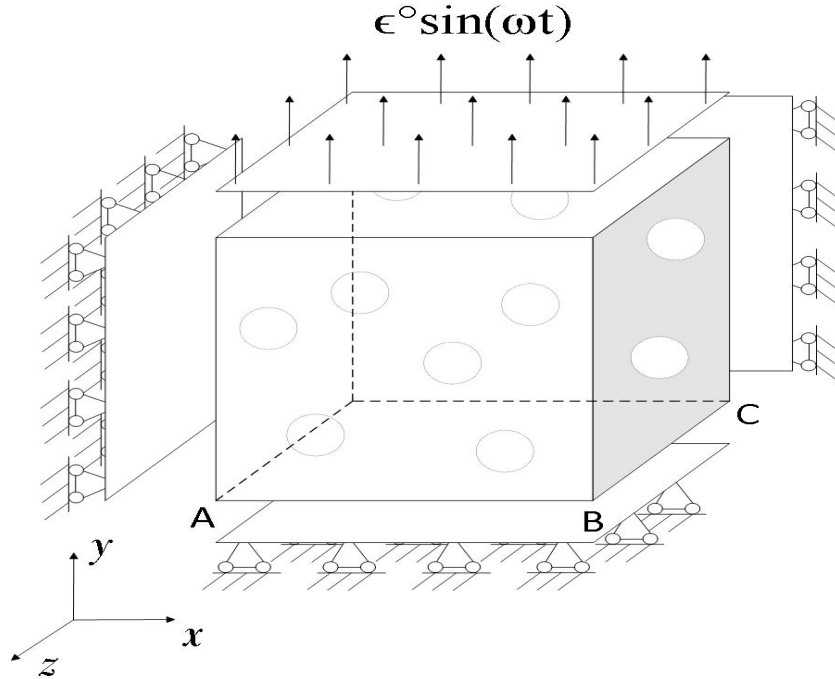


Figure 4.6: Boundary conditions for model with spherical inclusions.

Abaqus hexahedral element C3D20 and tetrahedral element C3D10 were used for meshing of matrix. Inclusion and interphase were meshed using the tetrahedral element C3D10. The mesh size was decreased from 0.03 mm gradually to determine the variation in $\tan \delta$. No significant change in the ensemble averaged $\tan \delta$ value was noticed. Table 4.1 lists the dimension and mesh size used for the finite element model. The average mesh seed size of the spherical inclusion and matrix is 0.015 mm. Seed size for interphase is 0.0015 mm. A finer seed size increased the computational requirements of the model without any noticeable change in the damping values.

4.1.2 Boundary and Loading Conditions

The damping properties of the composites is calculated by generating appropriate constraints and displacements for the model using mixed boundary conditions. Mixed boundary condition provide a simplified and accurate solution for models with complex and fine meshing patterns. In general, solving such problems requires a combination of linear displacement boundary condition, uniform traction boundary

condition and periodic boundary condition. To avoid complexity in the composite model, this study only used mixed boundary conditions with linear displacement.

A normal strain is applied to the top surface of the RVE. Roller supports are applied on the left, back and bottom surface. These supports restrict the displacement of left, bottom and back surfaces in x, y and z direction respectively. The figure 4.6 shows a representation of the boundary conditions. The z component of displacement of the front face of the RVE is tied to the edge AB and the x component of displacement of the right face is tied to edge BC. This is done to prevent any planar distortion in the model upon application of strain on the top surface. The loading frequency is varied from 10^{-8} /s to 10^2 /s. The above mentioned boundary conditions are applied to different inclusion distribution configuration of the polymer model. Damping properties for each configuration is calculated over the range of frequency while keeping the amplitude of the loading strain the same.

4.2 Composite with Carbon Nanotube Inclusions

The second part of the study deals with modeling and analysis of a carbon nanotube polymer composite model. This model consists of hollow single wall carbon nanotubes inserted in a matrix. The carbon nanotubes are elastic in nature with very high elastic modulus as compared to the matrix. The matrix is in shape of a cuboid with two dimensions significantly larger than the third. The inclusions are in shape of hollow tubes which are sinusoidal in nature. The wavelength and amplitude combinations used to model the inclusions are listed in table ???. Here, ' d ' refers to the diameter of the nanotube inclusions, ' a ' refers to the amplitude and ' λ ' is the wavelength. Waviness is calculated as the ratio of amplitude over wavelength. The outer surface of the inclusion is tied to surrounding matrix using 'tie' function of ABAQUS.

Abaqus hexahedral element C3D20 and tetrahedral element C3D10 were used for matrix mesh with seed size 3 nm. Carbon nanotube inclusions are modelled using ABAQUS shell element S4. This element is ideal for calculations involving thin but

stiff material response. Seed size of 1 nm was used for meshing of nanotube inclusions. A further reduction in seed size increased the computational requirements without a noticeable impact on the $\tan \delta$ response of the polymer.

Table ?? lists all the dimensions used for modeling the RVE. All the dimensions are in nanometers. The study analyzes the effect of inclusion waviness, volume fraction and loading frequency on the damping properties of the polymer.

Table 4.2: SWCNT Polymer Matrix Parameters [3]

d	V_f	a	λ	a/λ	H	W	t
20	5	330	1320	0.25	1770	1400	50
20	5	264	1320	0.2	1800	1350	45
20	5	200	1320	0.5	1770	920	50
20	5	132	1320	0.1	1750	1300	40
20	5	80	1320	0.06	1700	1200	40
20	5	66	1320	0.05	1770	550	35
10	5	145	1320	0.1	1770	650	30
10	5	198	1320	0.15	1700	800	32
10	5	264	1320	0.2	1700	800	32
10	5	330	1320	0.25	1700	1000	32

4.2.1 Boundary and Loading Conditions

The second part of the study also utilizes mixed boundary conditions for predicting the damping capability of the polymer. The RVE is in shape of a cuboid with two dimensions significantly larger than the third dimension. Figure 4.7 is a 2D representation of boundary conditions used on the model. For the polymer with nanotube inclusion, the roller supports are applied on bottom, right and back surface of the model. These roller supported faces are restricted to move in y , x and z directions respectively.

This study attempts to analyse the effect of change in loading directions on the damping properties of the polymer composite. The carbon nanotube inclusions are dispersed in the matrix in such a way that the orientation is along the direction of periodic loading. In other cases tested in this study, an attempt has been made to

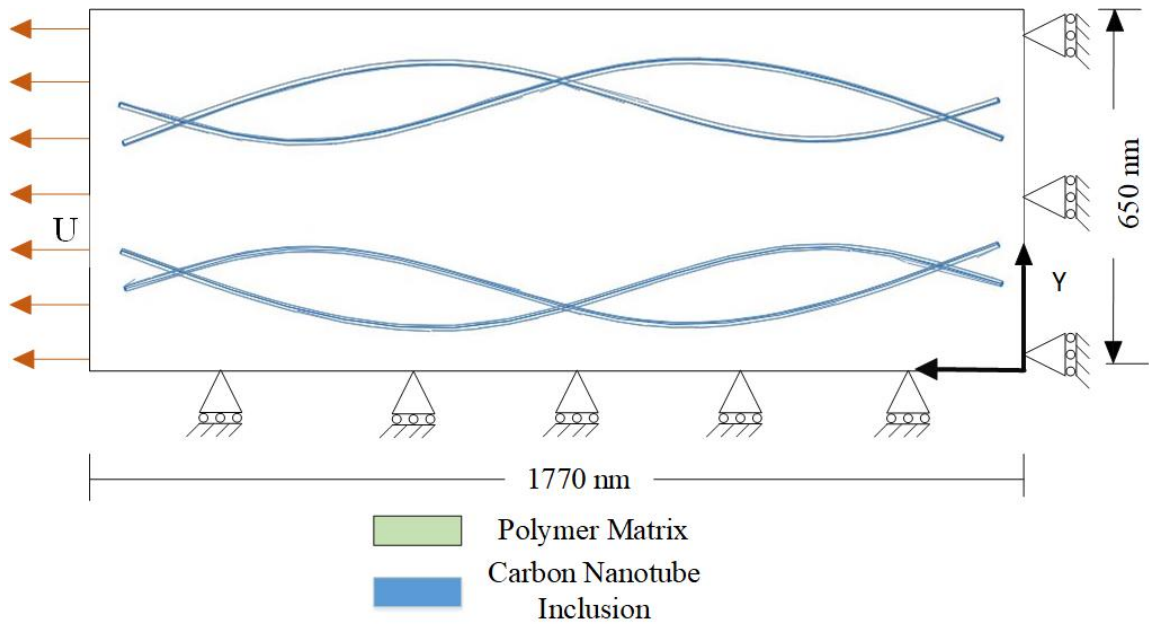


Figure 4.7: Boundary conditions for polymer with nanotube inclusions.

notice any change in the damping properties when the orientation of the nanotubes is perpendicular to the direction of load. This study analysis the effect of loading direction by keeping the orientation of the nanotubes same while changing the loading strain direction.

CHAPTER 5: RESULT AND DISCUSSION

This section contains the results and discussions relate to different cases under consideration. The graphs are a representation of variation of $\tan \delta$ over a range of frequency. The first section deals with the results and discussion of polymer composite with spherical inclusions. The second part has the results and discussion for carbon nanotube polymer composite.

5.1 Polymer Composite with Spherical Inclusions

As discussed in the previous sections, polymer composite model is subjected mixed boundary conditions with a periodic loading on one of the faces. Damping capability of polymer model with and without interface is compared to determine the effect of interphase region on the damping capability of the polymer model.

5.1.1 Effect of Volume Fraction

In this section, the effect of volume fraction of the elastic inclusions on the overall damping capability of the polymer is studied. The study was conducted on three different volume fractions of 5% , 10% and 15%. Figure 5.1 shows the variation in damping capability of 5% inclusion polymer with and without interphase over a range of frequency. The figure suggests that there is minimal change in damping capability of the polymer upon addition of interphase. No change in damping capability is observed for low and high end of the frequency spectrum. The effect of interphase on the damping capability can only be noticed at the peak which is not significant for 5% inclusion volume fraction.

Figure 5.2 shows the variation in damping capability of the polymer with 10% inclusion over a range of frequency. The damping capability of polymer with and

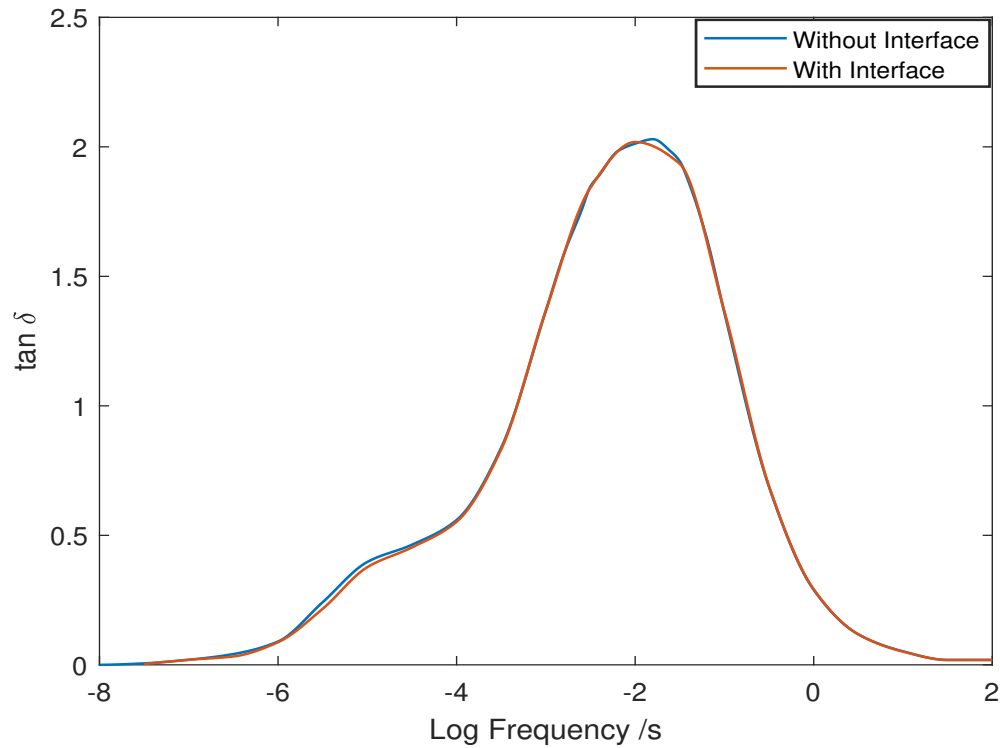
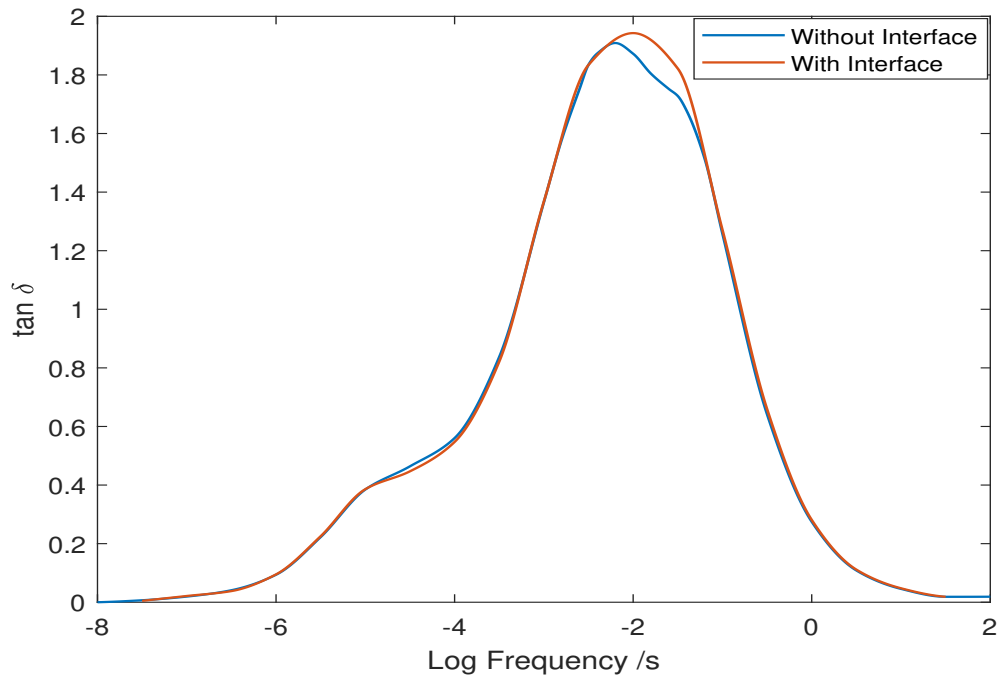
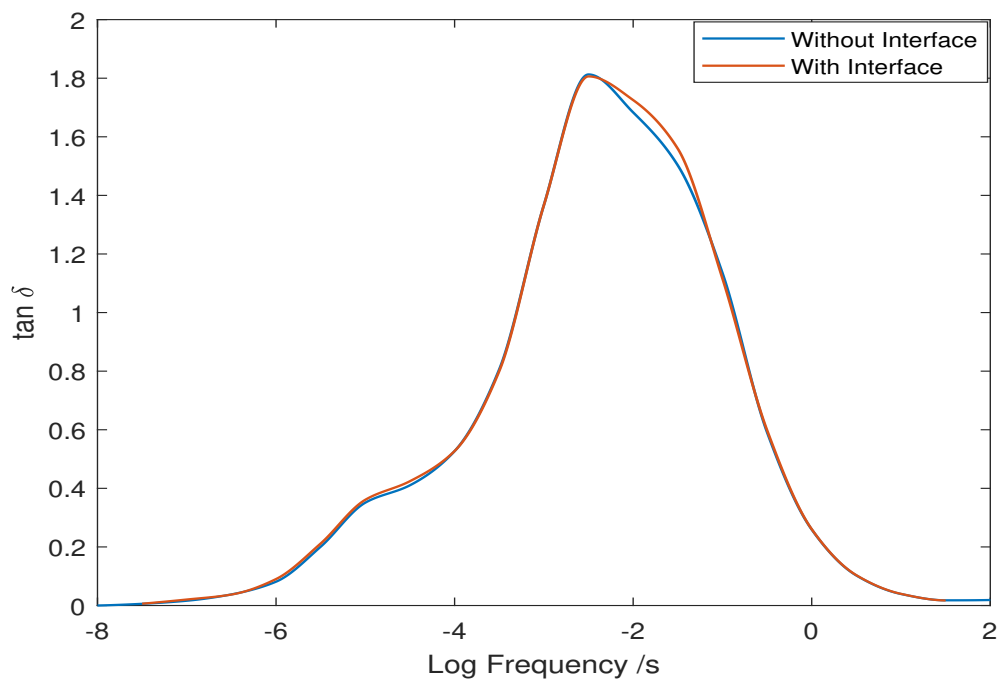


Figure 5.1: $\tan \delta$ for Volume Fraction 5%

without interphase is compared and a slight increment in the $\tan \delta$ value is observed at the peak frequency of $10^{-2}/s$. Figure 5.3 graph shows the variation in damping capability of the polymer with 15% inclusion over a range of frequency. An acute peak is observed in the damping response of polymer with 15% inclusions. Unlike the response of polymers with 10% volume fraction and lower, the damping peak is concentrated at a peak value of $10^{-1}/s$. Minimal change in damping capability is observed on increasing the volume fraction.

From above results it is concluded that the interphase has minimal effect on the damping capability of the polymer composites with 5% and 15% inclusion volume fraction. Slight increment in peak damping capability is observed for polymer model with 10% inclusion volume fraction. The interphase thickness remains constant in each case.

Figure 5.2: $\tan \delta$ for Volume Fraction 10%Figure 5.3: $\tan \delta$ for Volume Fraction 15%

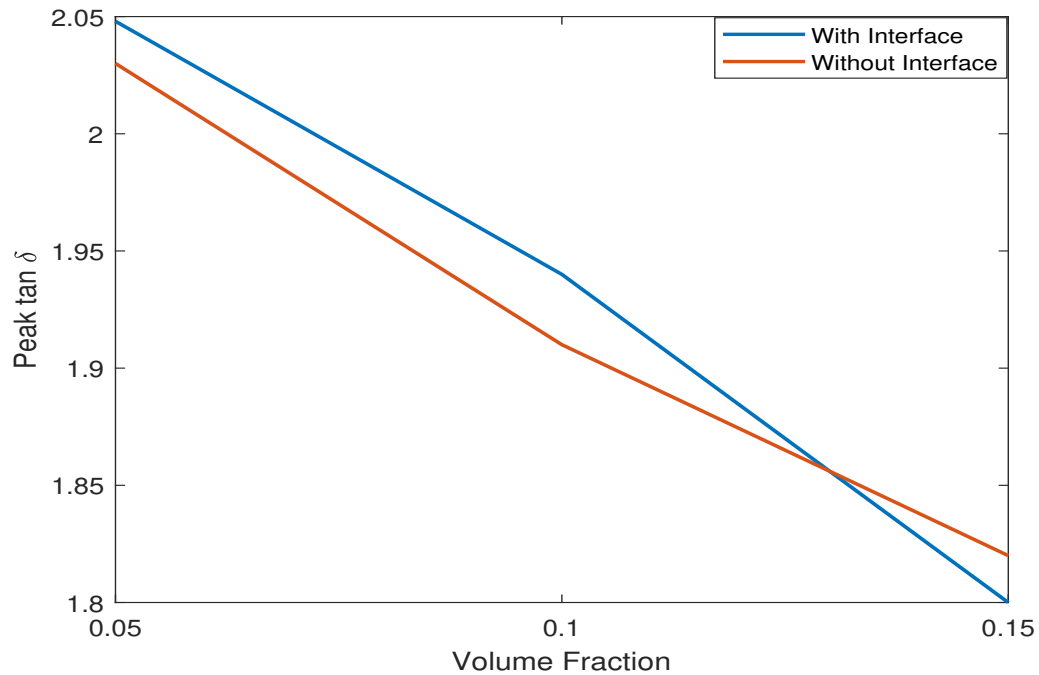


Figure 5.4: Comparison of peak $\tan \delta$ with and without interphase against volume fraction

5.1.2 Effect of Interphase

Figure 5.4 compares the peak value of $\tan \delta$ for all three volume fractions of 5, 10 and 15%. A slight increment in damping capability upon addition of interphase layer is observed.

5.1.3 Ensemble Averaging

The first part of the study consists of polymer with spherical inclusions randomly dispersed in a viscoelastic matrix. The study uses Random Sequential Absorption technique for dispersion of inclusions within the matrix. Ensemble averaging is performed to study the effect of randomness on predicting the peak damping capability of the polymer model. The damping capability of polymer model with a specific volume fraction is calculated by taking an ensemble average of 20 different RVEs. Each of these instances have same inclusion volume fraction but the arrangement of inclusion within the cuboidal matrix is different. This study shows how increasing

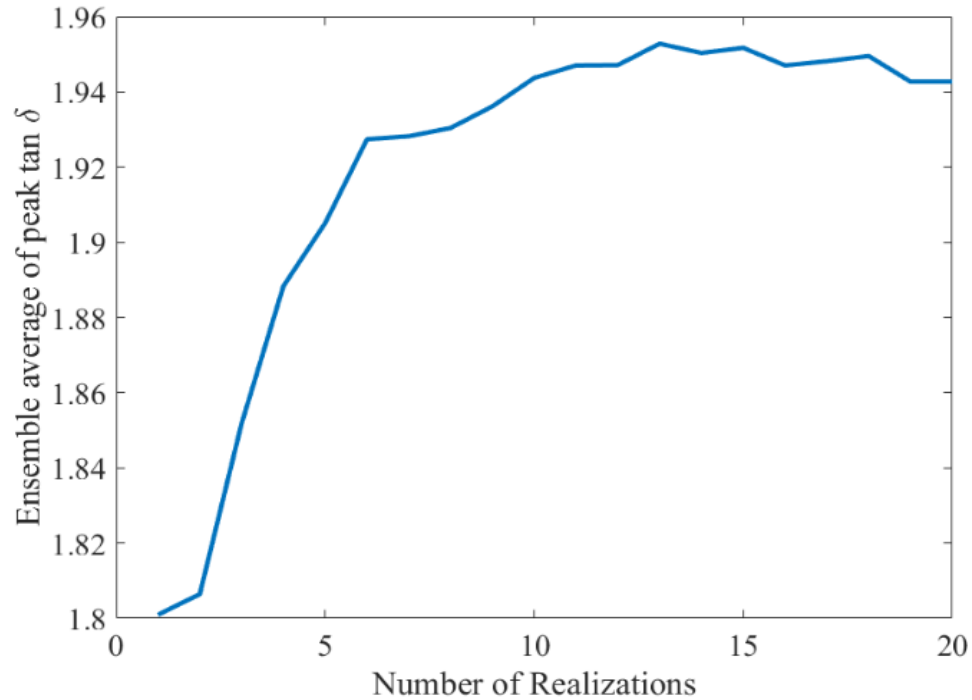


Figure 5.5: Ensemble Averaging for polymer with 5% volume fraction.

the number of instance affects variation in peak damping capability prediction of the polymer composite.

Figure 5.5 shows that as the number of instances taken into consideration increases, the deviation in peak $\tan \delta$ decreases. The figure shows the average of 20 iterations of model with same volume fraction, boundary and loading conditions but different inclusion positioning.

5.2 Carbon Nanotube Polymer Composite

This section maps the response of carbon nanotube polymers with different volume fraction over a range of frequency. It is noticed that with loading and boundary conditions same, the nature of response for the carbon nanotube polymer is similar to that of spherical inclusion polymer. This is due to the same visco elastic nature of the matrix. However, a reduction in peak $\tan \delta$ values is noticed as carbon nanotubes are used as inclusions for determining the damping capability of the polymer composite model.

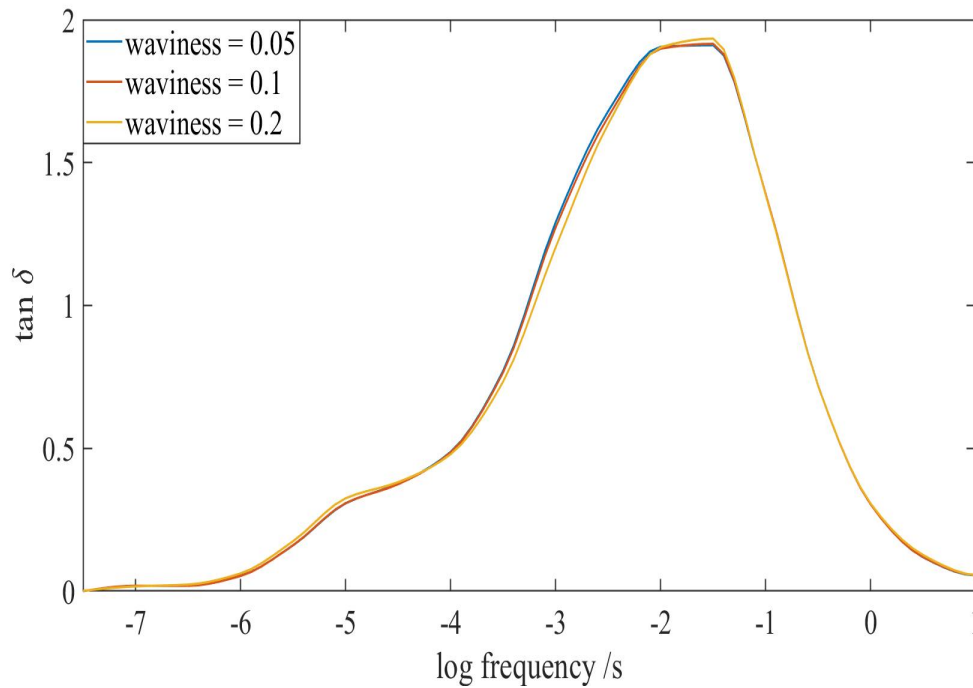


Figure 5.6: $\tan \delta$ response with 5% volume fraction.

5.2.1 Effect of Waviness

Figure 5.6 represents the damping response of polymer composite with 5% inclusion volume fraction. The waviness of the inclusions was changed while keeping the volume fraction same. It can be noticed that at this volume fraction, the change in waviness does not have a significant change on the damping capability of the composite.

Figure 5.7 shows the $\tan \delta$ response for polymer with 10% nanotube inclusions. It is noticed that as the volume fraction increases the peak $\tan \delta$ for the polymer reduces. However, the inclusion waviness has a slight impact on damping property of the polymer model. Figure 5.8 shows a similar trend in the damping response for polymer with 15% inclusion volume fraction. A slight reduction in peak damping capability is noticed as the waviness of the inclusions is increased while keeping the volume fraction same. It is noticed that the damping response for all volume fractions is identical for low and high end of the frequency range.

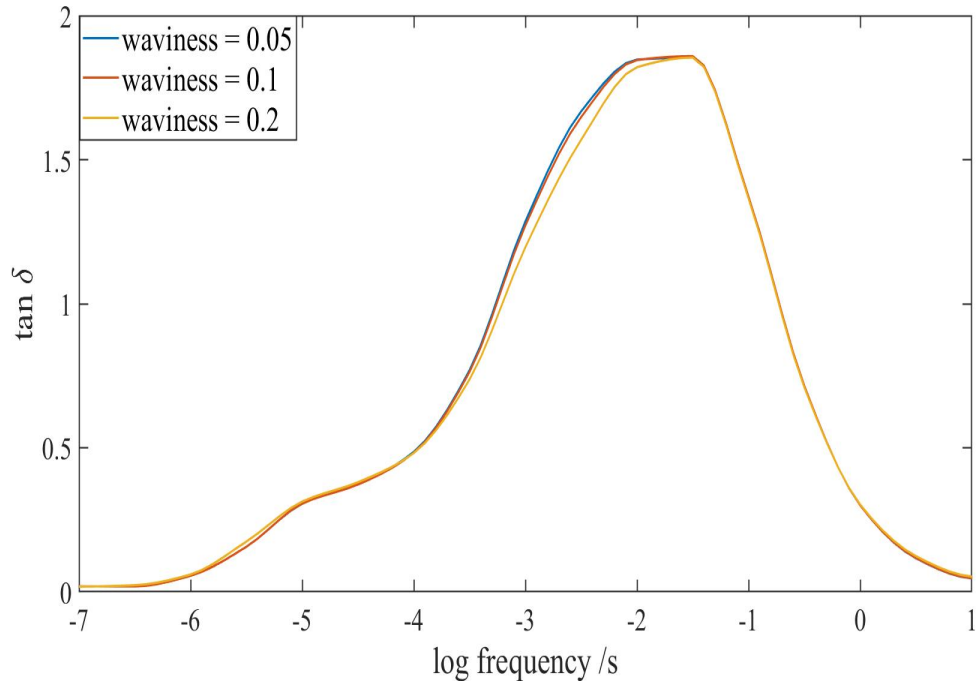


Figure 5.7: $\tan \delta$ response with 10% volume fraction.

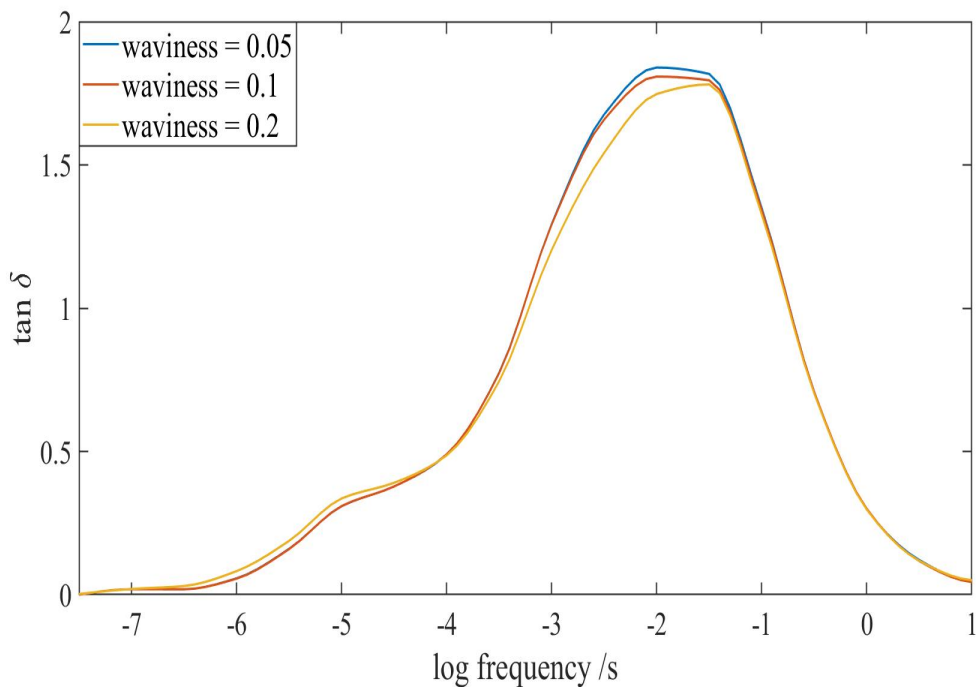


Figure 5.8: $\tan \delta$ response with 15% volume fraction.

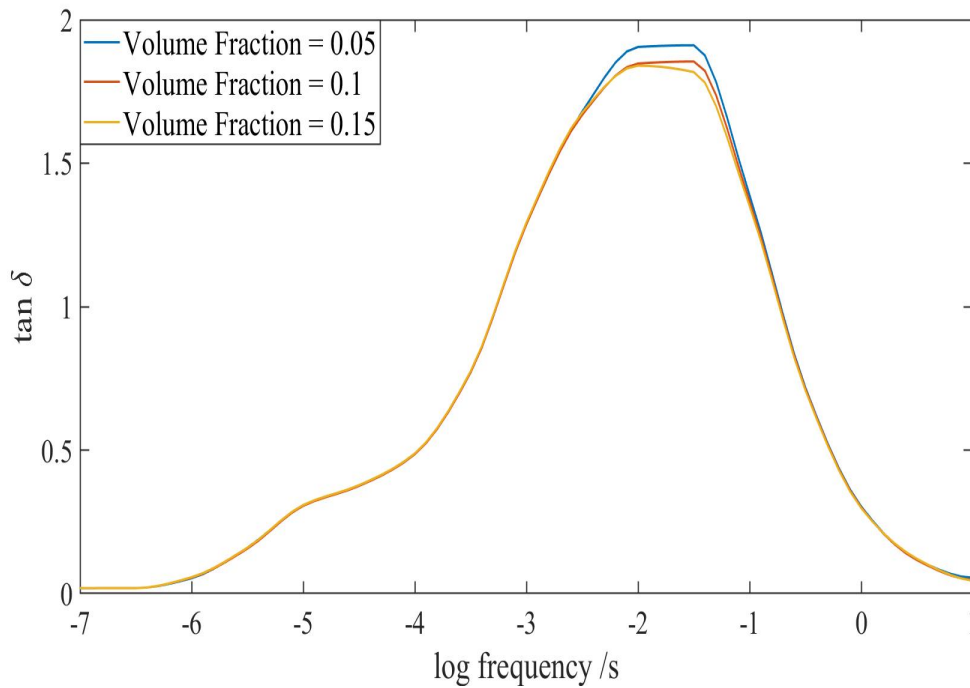


Figure 5.9: $\tan \delta$ response for 0.05 waviness against all volume fraction.

5.2.2 Effect of Volume Fraction

This section lays out the effect of volume fraction by comparing the damping response of models with same waviness but increasing volume fraction. The polymer models are studied for inclusion volume fraction 5%, 10% and 15% with waviness as 0.05, 0.1 and 0.2.

Figure 5.9 shows the damping response of polymer model with 0.05 waviness. The inclusion volume fraction is increased while keeping the waviness same. As the volume fraction is increased, the damping capability of the model reduces. This change in damping capability is only noticed at frequencies corresponding to peak $\tan \delta$ values of the model.

Figure 5.10 shows the damping response for polymer with waviness 0.1 against increasing volume fraction. As the volume fraction is increased, the peak damping capability of the model reduces. A slight reduction in $\tan \delta$ value is observed at peak frequency with no significant change in damping capability at other frequencies

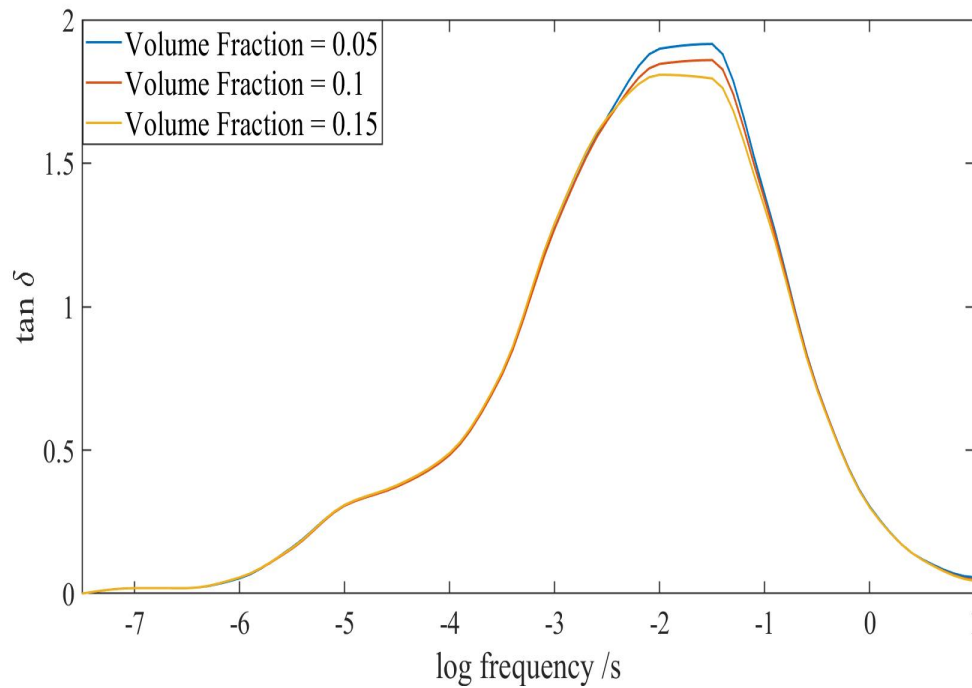


Figure 5.10: $\tan \delta$ response for 0.1 waviness against all volume fraction.

within the range.

Figure 5.11 shows the damping response for polymer with waviness 0.2 against all volume fraction. It is observed that the peak damping capability of models with waviness 0.05, 0.1 and 0.2 reduces as the volume fraction is increased. No change on damping capability is observed upon changing the input parameters for frequencies near the low and high end of the range.

In figure 5.12, the peak $\tan \delta$ of all volume fraction is compared against different waviness. It can be observed that the peak $\tan \delta$ response of the models reduces considerable for inclusion volume fraction 5%. The $\tan \delta$ response for waviness 0.05 straightens out as the volume fraction is increased. A similar observation is made for waviness 0.1 and 0.2. However, for waviness 0.1 and 0.2, the $\tan \delta$ response further reduces as the volume fraction is increased from 5% to 15%.

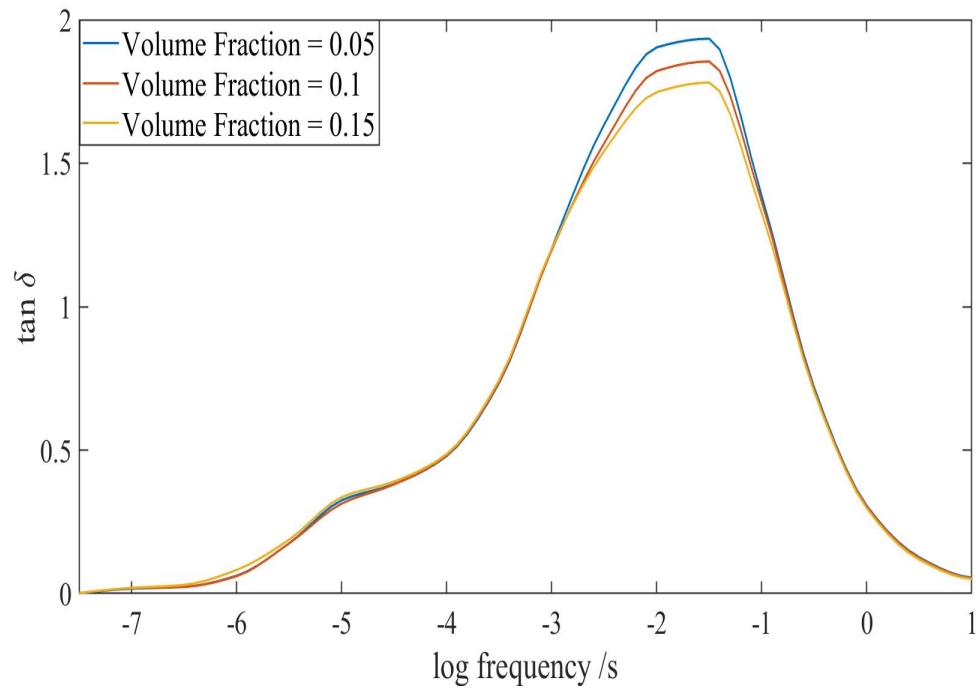


Figure 5.11: $\tan \delta$ response for 0.2 waviness against all volume fraction.

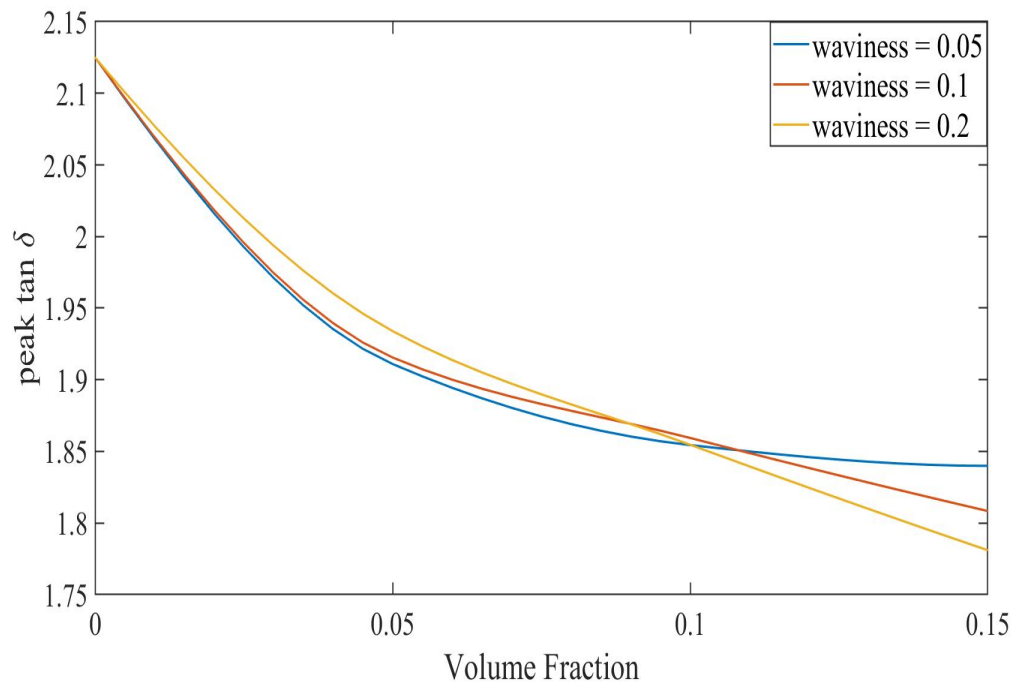


Figure 5.12: Comparison of peak $\tan \delta$.

5.3 Sensitivity Analysis

A sensitivity analysis was performed to determine the change in damping capability of the composite models upon changing the input parameters of material properties like elastic modulus of matrix and inclusions. The analysis was conducted for polymer composite models with 5% nanotube inclusions volume fraction and waviness of 0.05, 0.1 and 0.2. The elastic Young's modulus for the inclusions and the matrix is varied within a range to study the change in peak damping capability. This study uses stratified sampling technique called Latin Hypercube Sampling (LHS)[26] to generate random samples for the sensitivity analysis. LHS is a statistical method to generate random samples within a multidimensional data set. It is based on a Latin square which is a square grid containing only one sample in each row and column. Latin hypercube sampling technique extends this to multidimensional data set. For sampling of 'n' number of variables, each variable is divided into 'm' equal intervals. These intervals are distributed to satisfy the Latin hypercube requirements. A random samples are picked from each of these intervals which results in equal number of samples for each variable.

Table 5.1: Parameter range for sensitivity analysis.

Part	Variation	Unit
Matrix	9.4 to 960	MPa
Inclusion	0.5 to 1.5	TPa

One of the main advantages of using LHS technique is that the number of sample does not increase for increase in number of dimensions/variables. This saves computational time and cost for an effective analysis. The sections below show the results for sensitivity analysis of the three models. This study used LHS technique to generate 100 samples of inclusion and matrix modulus within the assigned range. Table 5.1

lists the range of variation for matrix and inclusion modulus. The inclusion modulus is varied from -50% to +50% of 1 TPa

Figure 5.13 shows a scatter plot distribution of peak damping capability against variation in matrix modulus. A quadratic curve is fit to the distribution using the depicted equation. It is observed that as the elastic modulus is increased from 9.4 MPa, the peak damping capability increases and the curve flattens out as the matrix stiffness is increased further. Figure 5.14 shows the scatter plot for variation in inclusion modulus. The graph suggests that the peak damping capability of the model decreases as the inclusions are made stiffer. It is noticed that the distribution for inclusions is much more scattered than the matrix. A wider range of variation for inclusion modulus and more number of samples will give a more accurate view. Figure 5.15 shows the analysis result for waviness 0.1. It is observed that the peak damping capability increases up to a certain limit as the matrix is made stiffer. Figure 5.16 shows the analysis results for inclusion modulus. The damping capability reduces as the inclusions are made stiffer. It is noticed that the peak damping value for 0.1 waviness model is less than the 0.05 which again suggests decrease in peak damping capability as the waviness is increased. Figure 5.17 and 5.18 show the analysis result for model with waviness 0.2 against matrix and inclusion modulus respectively. A reduction in peak damping value for both matrix and inclusion is noticed.

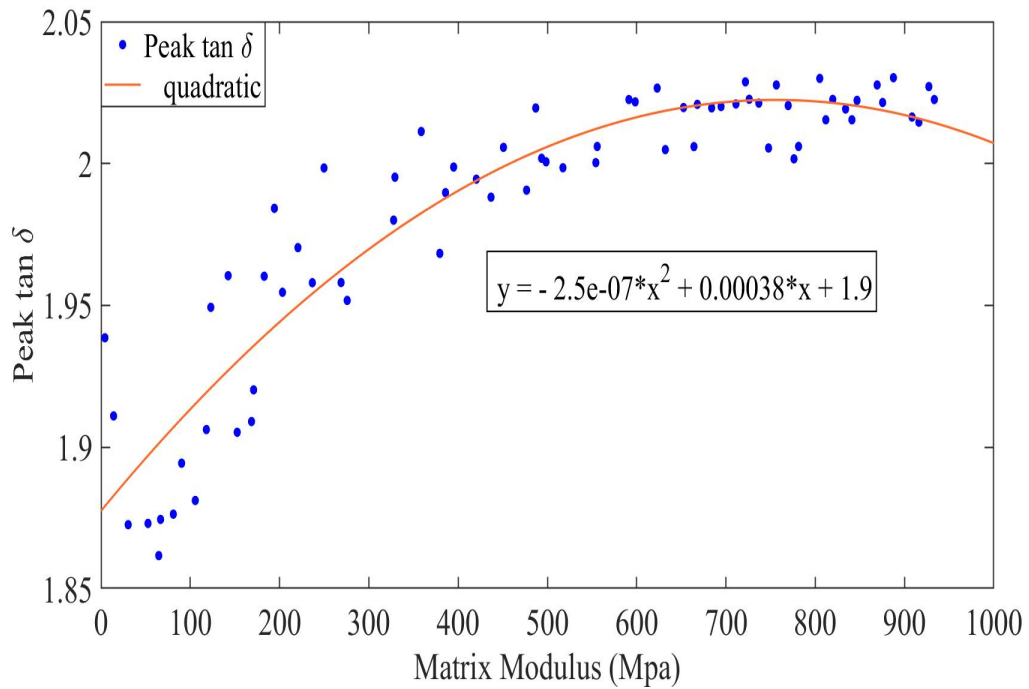


Figure 5.13: Sensitivity analysis against matrix modulus for volume fraction 5% and 0.05 waviness.

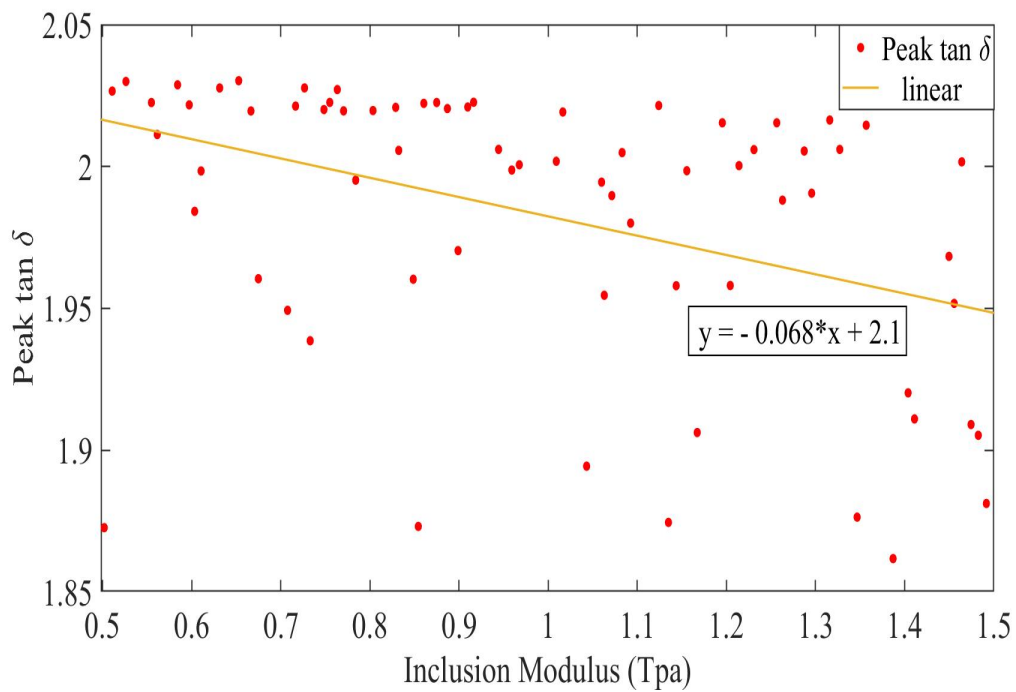


Figure 5.14: Sensitivity analysis against inclusion modulus for volume fraction 5% and 0.05 waviness.

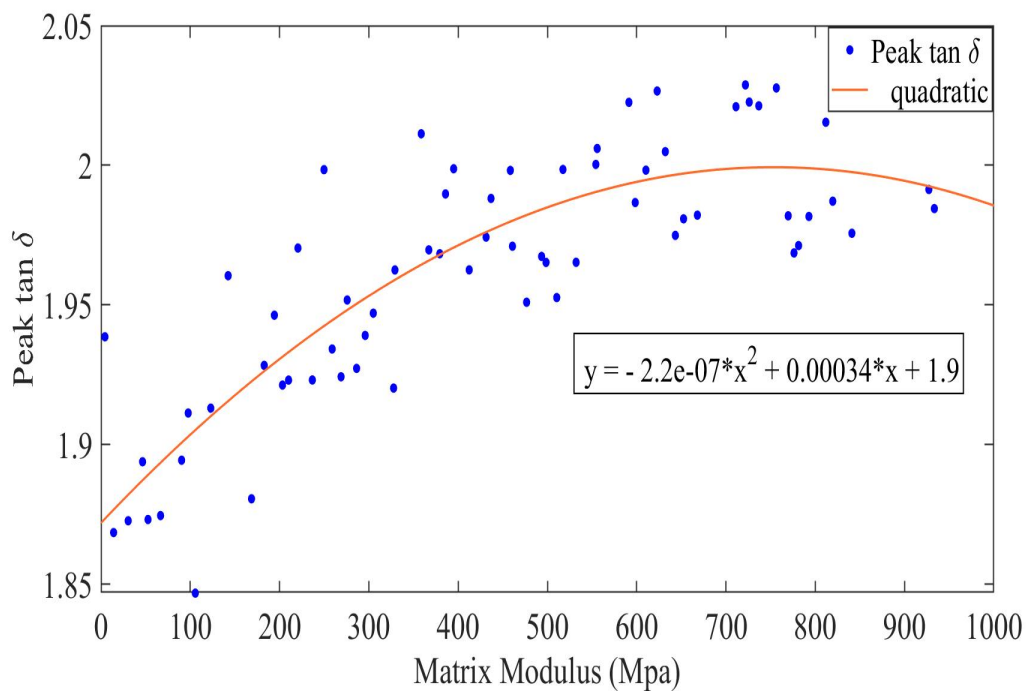


Figure 5.15: Sensitivity analysis against matrix modulus for volume fraction 5% and 0.1 waviness.

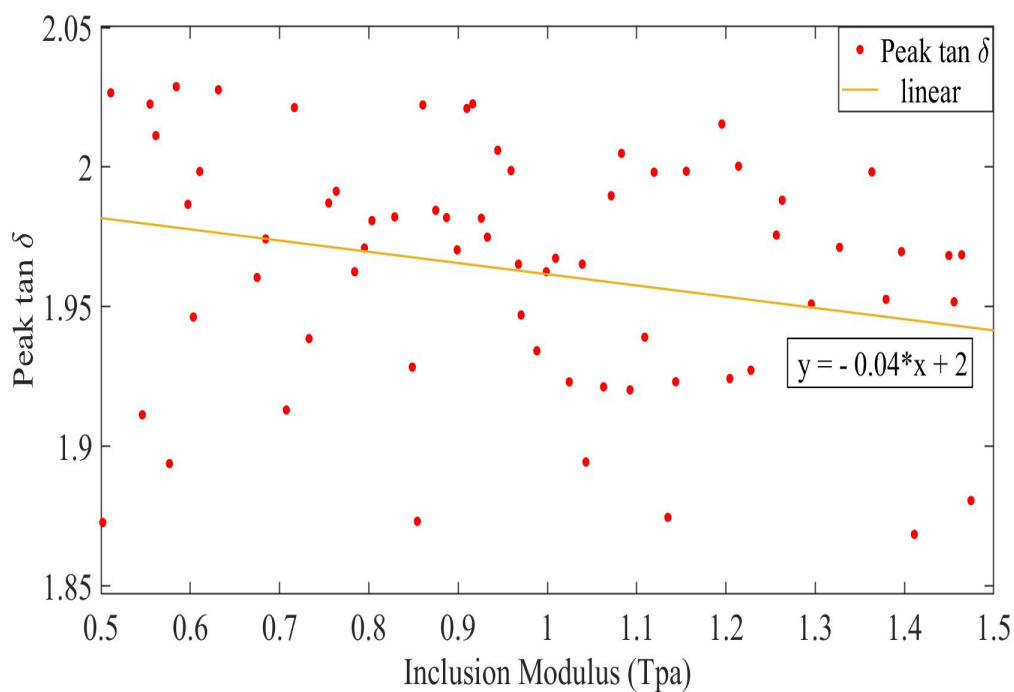


Figure 5.16: Sensitivity analysis against inclusion modulus for volume fraction 5% and 0.1 waviness.

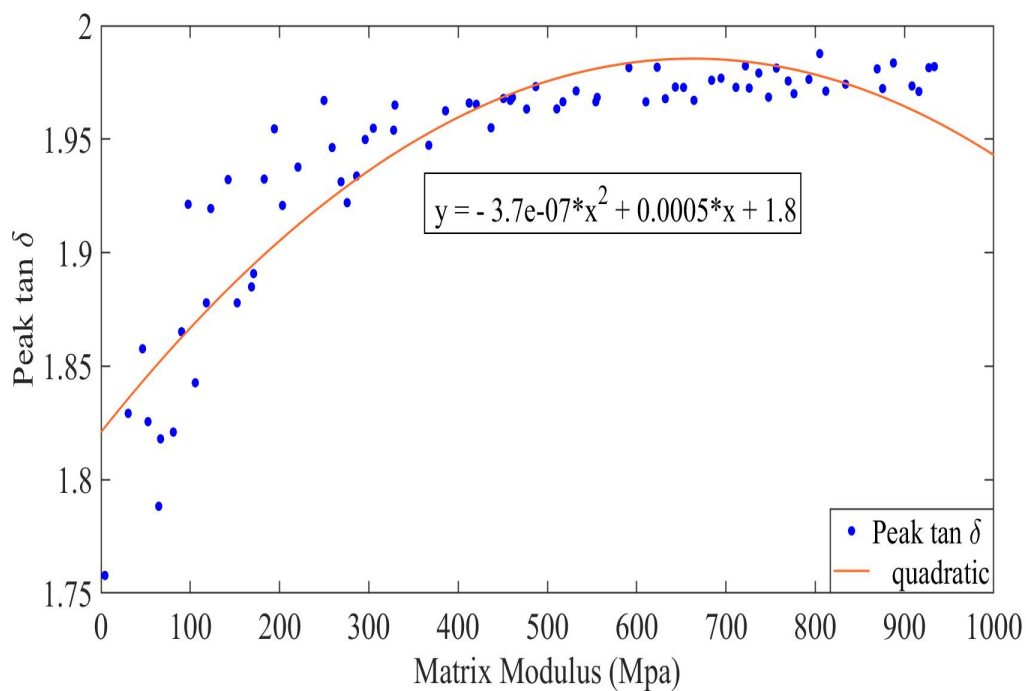


Figure 5.17: Sensitivity analysis against matrix modulus for volume fraction 5% and 0.2 waviness.

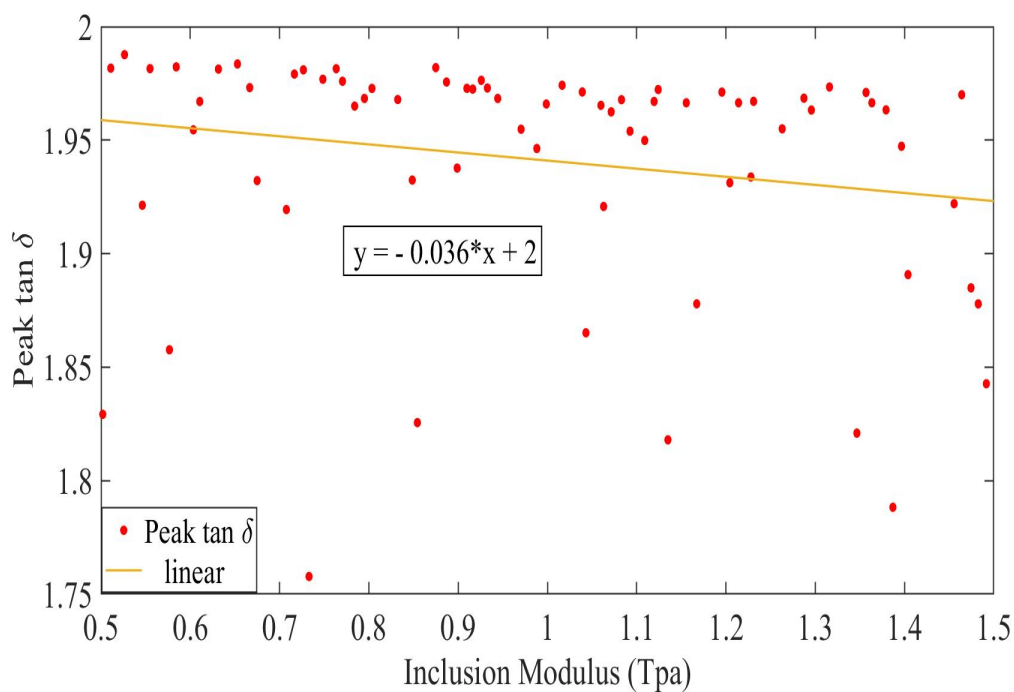


Figure 5.18: Sensitivity analysis against inclusion modulus for volume fraction 5% and 0.2 waviness.

CHAPTER 6: CONCLUSION

In this study the damping capability of two types of polymer composite models is analysed using finite element methods. The first composite is modelled as spherical glass inclusions in a viscoelastic matrix and the second composite is modelled as elastic single wall carbon nanotube inclusions in a viscoelastic matrix. The finite element models for both composites are subjected to mixed boundary conditions with normal strain on one of the faces. The damping capability is measured in terms of $\tan \delta$. The study analyzes the damping response of the models and how it is influenced by changing some key parameters like volume fraction and shape of inclusions, loading frequency, constituent material modulus etc. It is observed that the loading frequency has a profound affect on the damping capability of the models with peak at 10^2 /s.

Study of polymer model with glass inclusions showed that there is minimal change in damping capability of the model due to the viscoelastic interphase layer. A slight increment in damping capability is observed at volume fraction of 10%. Minimal increment in damping capability is observed for volume fraction 5% and 10%. Results show that the frequency of applied loading plays an important role in variation of $\tan \delta$ value. The value of $\tan \delta$ is close to zero for very low end as well as very high end frequency within the range. Damping capability is highest around the loading frequency of 10^2 /s. Study showed that the arrangement of inclusions within the matrix played an important role in determining the damping capability of the model. Ensemble averaging was used to study the effect of randomness on damping capability of the models. Study of composites model with elastic carbon nanotube inclusions was performed to analyze the effect of inclusion volume fraction, waviness and loading frequency. Study showed that for models with inclusion volume fraction 5 % and 10

% increase in inclusion waviness did not have a significant impact on the damping response of the composite model. For the model with 15% inclusion volume fraction, a slight reduction in damping capability is observed with increase in inclusion waviness. Waviness was calculated as a ratio of amplitude to waviness of the carbon nanotube inclusions. The study also showed that for a specific inclusion waviness, the damping capability of the model reduces with increase in volume fraction. This reduction is observed near the peak frequency which is $10^2/s$.

A sensitivity analysis helped in determining the change in peak damping capability of the model over a wide range of elastic modulus for both matrix and inclusions. The analysis was conducted for models with inclusion volume fraction 5 % and waviness of 0.05, 0.1 and 0.2. It is observed that the peak damping capability of the model increases with increase in matrix stiffness. In case of inclusions, the damping capability of the composite models decreases as the stiffness of the inclusions was increased. An overall reduction in peak damping capability was noticed as the waviness was increased while keeping the volume fraction.

REFERENCES

- [1] S. S. Kulkarni and A. Tabarraei, “A stochastic analysis of the damping property of filled elastomers,” *Macromolecular Theory and Simulations*, vol. 28, no. 2, p. 1800062, 2019.
- [2] L. C. Brinson and W. Lin, “Comparison of micromechanics methods for effective properties of multiphase viscoelastic composites,” *Composite Structures*, vol. 41, no. 3-4, pp. 353–367, 1998.
- [3] A. Pantano, G. Modica, and F. Cappello, “Multiwalled carbon nanotube reinforced polymer composites,” *Materials Science and Engineering: A*, vol. 486, no. 1-2, pp. 222–227, 2008.
- [4] C. W. Roeder and J. F. Stanton, “Elastomeric bearings: state-of-the-art,” *Journal of Structural Engineering*, vol. 109, no. 12, pp. 2853–2871, 1983.
- [5] M. D. Rao, “Recent applications of viscoelastic damping for noise control in automobiles and commercial airplanes,” *Journal of Sound and Vibration*, vol. 262, no. 3, pp. 457–474, 2003.
- [6] C. Tsai and H. Lee, “Applications of viscoelastic dampers to high-rise buildings,” *Journal of structural engineering*, vol. 119, no. 4, pp. 1222–1233, 1993.
- [7] T. V. Duncan, “Applications of nanotechnology in food packaging and food safety: barrier materials, antimicrobials and sensors,” *Journal of colloid and interface science*, vol. 363, no. 1, pp. 1–24, 2011.
- [8] R. Adams and D. Bacon, “Effect of fibre orientation and laminate geometry on the dynamic properties of cfrp,” *Journal of Composite Materials*, vol. 7, no. 4, pp. 402–428, 1973.
- [9] S. Hwang and R. Gibson, “Micromechanical modeling of damping in discontinuous fiber composites using a strain energy/finite element approach,” *Journal of engineering materials and technology*, vol. 109, no. 1, pp. 47–52, 1987.
- [10] M. Kaliske and H. Rothert, “Damping characterization of unidirectional fibre reinforced polymer composites,” *Composites Engineering*, vol. 5, no. 5, pp. 551–567, 1995.
- [11] T. Mori and K. Tanaka, “Average stress in matrix and average elastic energy of materials with misfitting inclusions,” *Acta metallurgica*, vol. 21, no. 5, pp. 571–574, 1973.
- [12] S. S. Kulkarni, A. Tabarraei, and P. P. Ghag, “A finite element approach for study of wave attenuation characteristics of epoxy polymer composite,” in *ASME 2018 International Mechanical Engineering Congress and Exposition*, pp. V009T12A042–V009T12A042, American Society of Mechanical Engineers, 2018.

- [13] S. S. Kulkarni and A. Tabarraei, "Study of damping properties of polymer matrix composites through wave propagation," in *ASME 2017 International Mechanical Engineering Congress and Exposition*, pp. V001T03A018–V001T03A018, American Society of Mechanical Engineers, 2017.
- [14] S. S. Kulkarni, A. Tabarraei, and P. P. Ghag, "A finite element approach for study of wave attenuation characteristics of epoxy polymer composite," in *ASME 2018 International Mechanical Engineering Congress and Exposition*, pp. V009T12A042–V009T12A042, American Society of Mechanical Engineers, 2018.
- [15] F. Fisher and L. Brinson, "Viscoelastic interphases in polymer–matrix composites: theoretical models and finite-element analysis," *Composites Science and Technology*, vol. 61, no. 5, pp. 731–748, 2001.
- [16] D. Qian, G. J. Wagner, W. K. Liu, M.-F. Yu, and R. S. Ruoff, "Mechanics of carbon nanotubes," *Applied Mechanics Reviews*, vol. 55, no. 6, pp. 495–533, 2002.
- [17] J. Bernholc, D. Brenner, M. Buongiorno Nardelli, V. Meunier, and C. Roland, "Mechanical and electrical properties of nanotubes," *Annual Review of Materials Research*, vol. 32, no. 1, pp. 347–375, 2002.
- [18] H. Qi, K. Teo, K. Lau, M. Boyce, W. Milne, J. Robertson, and K. Gleason, "Determination of mechanical properties of carbon nanotubes and vertically aligned carbon nanotube forests using nanoindentation," *Journal of the Mechanics and Physics of Solids*, vol. 51, no. 11-12, pp. 2213–2237, 2003.
- [19] R. Andrews, D. Jacques, M. Minot, and T. Rantell, "Fabrication of carbon multi-wall nanotube/polymer composites by shear mixing," *Macromolecular Materials and Engineering*, vol. 287, no. 6, pp. 395–403, 2002.
- [20] H. Xia, Q. Wang, K. Li, and G.-H. Hu, "Preparation of polypropylene/carbon nanotube composite powder with a solid-state mechanochemical pulverization process," *Journal of Applied Polymer Science*, vol. 93, no. 1, pp. 378–386, 2004.
- [21] Y. S. Song and J. R. Youn, "Influence of dispersion states of carbon nanotubes on physical properties of epoxy nanocomposites," *Carbon*, vol. 43, no. 7, pp. 1378–1385, 2005.
- [22] G. Odegard, T. Gates, K. Wise, C. Park, and E. Siochi, "Constitutive modeling of nanotube–reinforced polymer composites," *Composites Science and Technology*, vol. 63, no. 11, pp. 1671–1687, 2003.
- [23] R. Bradshaw, F. Fisher, and L. C. Brinson, "Fiber waviness in nanotube-reinforced polymer compositesii: modeling via numerical approximation of the dilute strain concentration tensor," *Composites Science and Technology*, vol. 63, no. 11, pp. 1705–1722, 2003.

- [24] F. Fisher, R. Bradshaw, and L. Brinson, “Effects of nanotube waviness on the modulus of nanotube-reinforced polymers,” *Applied Physics Letters*, vol. 80, no. 24, pp. 4647–4649, 2002.
- [25] A. Version, “6.13, analysis users manual,” *Dassault Systemes Simulia Corp., Providence, RI*, 2013.
- [26] M. D. McKay, R. J. Beckman, and W. J. Conover, “Comparison of three methods for selecting values of input variables in the analysis of output from a computer code,” *Technometrics*, vol. 21, no. 2, pp. 239–245, 1979.